

# Probing CP Violation in $\gamma\gamma \rightarrow W^+W^-$ with Polarized Photon Beams

S.Y. Choi and K. Hagiwara

*Theory Group, KEK, Tsukuba, Ibaraki 305, Japan*

and

M.S. Baek

*Department of Physics and Center for Theoretical Physics*

*Seoul National University, Seoul 151-742, Korea*

## Abstract

We demonstrate in a general framework that polarized photons by backscattered laser beams of adjustable frequencies at a TeV linear  $e^+e^-$  collider provide us with a very efficient mechanism to probe CP violation in two-photon collisions. CP violation in the process  $\gamma\gamma \rightarrow W^+W^-$  is investigated in detail with linearly polarized photon beams. There are two useful CP-odd asymmetries that do not require detailed information on  $W$  decay products. The sensitivity to the CP-odd form factors are studied quantitatively by assuming a perfect  $e\text{-}\gamma$  conversion and the  $20 \text{ fb}^{-1}$   $e^+e^-$  integrated luminosity at the  $e^+e^-$  c.m. energies  $\sqrt{s} = 0.5$  and 1.0 TeV. The sensitivity is so high that such experiments will allow us to probe new CP violation effects beyond the limits from some specific models with reasonable physics assumptions. We find that a counting experiment of  $W^+W^-$  events in the two-photon mode with adjustable laser frequencies can have much stronger sensitivity to the CP-odd  $\gamma(\gamma)WW$  form factors than can a  $W^+W^-$  decay-correlation experiment with a perfect detector achieve in the  $e^+e^-$  mode.

## I. INTRODUCTION

Even though the Standard Model (SM) has been successful in explaining all the experimental data up to date, it is believed that the SM is merely an effective theory valid at and below the weak scale and that new physics beyond the SM should appear at higher energies. We may expect to find new physics beyond the SM at high precision experiments on quantities whose SM values are suppressed. An interesting class of quantities where the SM contributions are strongly suppressed are those with CP violation. In the SM, CP violation stems from the complex phase of the Kobayashi-Maskawa (KM) quark-mixing matrix [1] and the size of CP violation is often extremely small. In contrast, various new physics scenarios on CP violation lead to comparatively large CP violation. Any CP-odd observable should hence be a good direct means to look for new physics effects.

The next generation of  $e^+e^-$  colliders [2] will offer interesting possibilities for studying physics of the heavy  $H$ ,  $t$ -quark, and the  $W$  bosons either in the  $e^+e^-$  mode or in the  $\gamma\gamma$  mode. Linear collider physics in the  $e^+e^-$  mode has been studied intensively for the past decade. Recently it has become clear that the  $\gamma\gamma$  mode (as well as the  $e\gamma$  mode) [3] can provide a good complement to experiments in the  $e^+e^-$  mode. For instance, it has been shown that the  $\gamma\gamma$  mode has a unique advantage in the determination of the Higgs-two-photon coupling [4] and its CP properties [5]. Pair production of the top-quark [6] and the  $W$  boson [7,8] in the  $\gamma\gamma$  mode has also been studied as probes of CP violation in physics beyond the SM. Most works [6,7] have concentrated on the use of the spin correlations of the pair-produced top-quarks and the  $W$  bosons which require detailed study of their decay products. Recently, it has been pointed out [9] that the (linearly)-polarized photon beams can provide us with very powerful tests of the top-quark electric dipole moment (EDM) without any information on the  $t\bar{t}$  decay patterns. Use of the  $\gamma\gamma$  mode with linearly polarized photon beams for studying CP violation in the process  $\gamma\gamma \rightarrow W^+W^-$  has also been considered by Bélanger and Coture [8].

In the present work we demonstrate in a rather general framework that polarized pho-

tons by backscattered laser beams of adjustable frequencies provide us with a very efficient mechanism to probe CP violation in the two-photon mode. We then give an extensive investigation of the possibility of probing CP violation with (linearly) polarized photon beams in the process  $\gamma\gamma \rightarrow W^+W^-$ . We extend in a systematic way the previous work [8] so as to cover an arbitrary angle between polarization directions of two photon beams and an arbitrary laser beam frequency. We find in particular that adjusting of the laser beam frequency is essential to optimize the sensitivity to CP violation phenomena. Furthermore, we study effects of all the possible dimension-six CP-odd operators composed of the Higgs doublet and the electroweak gauge bosons.

The  $W^+W^-$  production in the  $\gamma\gamma$  mode has several unique features in contrast to that in the  $e^+e^-$  mode,  $e^+e^- \rightarrow W^+W^-$ . In the  $e^+e^-$  mode, a pair of  $W$ 's are produced via an annihilation of the colliding  $e^-$  and  $e^+$  where the electronic chirality should be preserved along the electron line [10] due to the very small electron mass in the SM. This forces the positron helicity to be opposite to the electron helicity such that the initial  $e^+e^-$  configuration is always CP-even. On the contrary, there exists no apparent helicity selection mechanism in the  $\gamma\gamma$  production of  $W^+W^-$ . This feature makes any CP-odd  $\gamma\gamma$  configuration in the initial state a good probe of CP-violation in the two-photon mode.

The process  $\gamma\gamma \rightarrow W^+W^-$ , which is characterized by the angle between the  $W^+$  momentum and the  $\gamma$  momentum in the c.m. frame, and the helicities of the particles, is C, P and CP self-conjugate, when the particle helicities are averaged over. For this reason the helicities (but not all of them) need to be determined or statistically analyzed to observe violations of these discrete symmetries. One can take two approaches in analysing the process  $\gamma\gamma \rightarrow W^+W^-$ . One approach makes use of the spin correlations of the two decaying  $W$  bosons that can be measured by studying correlations in the  $W^+W^-$  decay-product system,  $(q\bar{q}')(l\bar{\nu})$  or  $(\bar{l}\nu)(l\bar{\nu})$ . The other method is to employ polarized photon beams to measure various polarization asymmetries of the initial states. Note that in the  $e^+e^-$  mode, only the former method, the spin correlations of final decay products, is available. The two-photon mode allows us to combine the two methods. The use of the former technique in the two-

photon collisions is essentially the same as that in  $e^+e^-$  collisions [11,13] with one crucial difference; in  $e^+e^-$  collisions the spin of the  $W^+W^-$  system is restricted to  $J \geq 1$ , while in  $\gamma\gamma$  collisions  $J = 0$  is allowed. For a specific final state such as  $W^+W^-$  and  $t\bar{t}$  the two-photon cross section is larger than the corresponding  $e^+e^-$  cross section. Especially, the  $W$  pair cross section in the two-photon mode is much larger than that in the  $e^+e^-$  mode because the  $\gamma\gamma$  mode has contributions from the  $J = 0$  channel near threshold and a  $t$ -channel  $W$  boson exchange. Moreover, it is easy to produce (linearly) polarized photon beams through the Compton back-scattering of polarized laser-light off the initial electron/positron beams. Hence the  $\gamma\gamma$  mode of future linear colliders provides some unique opportunities to probe CP violation.

In Section II we describe in a general framework how the photon polarization in the two-photon mode can be employed to study CP and  $\text{CPT}$  invariances. Here  $\tilde{T}$  is the so-called naive-time-reversal operation which reverses the signs of the three-momenta and spin of all particles but does not reverse the direction of the flow of time. The notation is introduced in Ref. [11]. Assuming that two-photon beams are purely linearly polarized in the colliding  $\gamma\gamma$  c.m. frame we construct two CP-odd and  $\text{CPT}$ -even asymmetries which allow us to probe CP violation without any direct information on the momenta and polarization of the final-state particles. All that we have to do is to count the number of signal events for a specific polarization configuration of the initial two photons. In Section III we give a short review of a mechanism of producing highly energetic photons, the Compton backscattering of laser photons off the electron/positron beam [14], and we introduce two functions that measure the partial transfers of the linear polarization from the laser beams to the Compton back-scattered photon beams. We then investigate in detail which parameters are crucial to optimize the observability of CP violation with linearly polarized laser beams.

In Section IV we study consequences of CP violating new interactions in the bosonic sector of the SM, by adopting a model-independent approach where we allow all six dimension-six operators of the electroweak gauge bosons and the Higgs doublet that are CP-odd [17]. We identify all the vertices and present the Feynman rules relevant for the process

$\gamma\gamma \rightarrow W^+W^-$ . In Section V, including all the new contributions, we present the helicity amplitudes of the  $\gamma\gamma \rightarrow W^+W^-$  reaction. Folding with the effective two-photon energy spectrum, we then estimate the size of the two CP-odd asymmetries for a set of CP-odd operator coefficients. In Section VI we present the  $1\text{-}\sigma$  sensitivities to the CP-odd parameters by assuming a perfect  $e\text{-}\gamma$  conversion in the Compton backscattering mechanism for an  $e^+e^-$  integrated luminosity of  $20\text{ fb}^{-1}$ . We then compare the sensitivities in the two-photon mode with those in the  $e^+e^-$  mode under the same luminosity and c.m. energy, by restricting ourselves to the  $W$  EDM and the  $W$  magnetic quadrupole moment (MQD). Finally in Section VII we summarize our findings and give conclusions.

## II. PHOTON POLARIZATION

In this section we fix our notation to describe in a general framework how photon polarization can provide us with an efficient mechanism to probe CP and  $\text{CPT}$  invariances in the two-photon mode. With purely linearly-polarized photon beams, we classify all the distributions according to their CP and  $\text{CPT}$  properties. Then, we show explicitly how linearly polarized photon beams allow us to construct two CP-odd and  $\text{CPT}$ -even asymmetries which do not require detailed information on the momenta and polarization of the final-state particles.

### A. Formalism

A photon should be transversely polarized. For the photon momentum in the positive  $z$  direction the helicity- $\pm 1$  polarization vectors are given by

$$|\pm\rangle = \mp \frac{1}{\sqrt{2}} (0, 1, \pm i, 0). \quad (2.1)$$

Generally, a purely polarized photon beam state is a linear combination of two helicity states and the photon polarization vector can be expressed in terms of two angles  $\alpha$  and  $\phi$  in a

given coordinate system as

$$|\alpha, \phi\rangle = -\cos(\alpha)e^{-i\phi}|+\rangle + \sin(\alpha)e^{i\phi}|-\rangle, \quad (2.2)$$

where  $0 \leq \alpha \leq \pi/2$  and  $0 \leq \phi \leq 2\pi$ . Then, the  $2 \times 2$  photon density matrix  $\rho$  [14,15] in the helicity basis  $\{|+\rangle, |-\rangle\}$  is given by

$$\rho \equiv |\alpha, \phi\rangle\langle\alpha, \phi| = \frac{1}{2} \begin{pmatrix} 1 + \cos(2\alpha) & -\sin(2\alpha)e^{2i\phi} \\ -\sin(2\alpha)e^{-2i\phi} & 1 - \cos(2\alpha) \end{pmatrix}. \quad (2.3)$$

It is easy to read from Eq. (2.3) that the degrees of circular and linear polarization are, respectively,

$$\xi = \cos(2\alpha), \quad \eta = \sin(2\alpha), \quad (2.4)$$

and the direction of maximal linear polarization is denoted by the azimuthal angle  $\phi$  in the given coordinate system. Note that  $\xi^2 + \eta^2 = 1$  as expected for a purely polarized photon. For a partially polarized photon beam it is necessary to rescale  $\xi$  and  $\eta$  by its degree of polarization  $P$  ( $0 \leq P \leq 1$ ) as

$$\xi = P \cos(2\alpha), \quad \eta = P \sin(2\alpha), \quad (2.5)$$

such that  $\xi^2 + \eta^2 = P^2$ .

Let us now consider the two-photon system in the center-of-mass frame where one photon momentum is along the positive  $z$  direction. The state vector of the two photons is

$$\begin{aligned} |\alpha_1, \phi_1; \alpha_2, \phi_2\rangle &= |\alpha_1, \phi_1\rangle |\alpha_2, -\phi_2\rangle \\ &= \cos(\alpha_1) \cos(\alpha_2) e^{-i(\phi_1 - \phi_2)} |++\rangle - \cos(\alpha_1) \sin(\alpha_2) e^{-i(\phi_1 + \phi_2)} |+-\rangle \\ &\quad - \sin(\alpha_1) \cos(\alpha_2) e^{i(\phi_1 + \phi_2)} |-+\rangle + \sin(\alpha_1) \sin(\alpha_2) e^{i(\phi_1 - \phi_2)} |--\rangle, \end{aligned} \quad (2.6)$$

and then the transition amplitude from the polarized two-photon state to a final state  $X$  in the two-photon c.m. frame is simply given by

$$\langle X|M|\alpha_1, \phi_1; \alpha_2, \phi_2 \rangle. \quad (2.7)$$

The azimuthal angles  $\phi_1$  and  $\phi_2$  are the directions of maximal linear polarization of the two photons, respectively, in a common coordinate system (see Fig. 1). In the process  $\gamma\gamma \rightarrow W^+W^-$ , the scattering plane is taken to be the  $x$ - $z$  plane in the actual calculation of the helicity amplitudes. The maximal linear polarization angles are then chosen as follows. The angle  $\phi_1$  ( $\phi_2$ ) is the azimuthal angle of the maximal linear polarization of the photon beam, whose momentum is in the positive (negative)  $z$  direction, with respect to the direction of the  $W^+$  momentum. Note that we have used  $|\alpha_2, -\phi_2\rangle$  in Eq. (2.6) for the photon whose momentum is along the negative  $z$  direction in order to employ a common coordinate system for the two-photon system.

For later convenience we introduce the abbreviation

$$M_{\lambda_1\lambda_2} = \langle X|M|\lambda_1\lambda_2 \rangle, \quad (2.8)$$

and two angular variables:

$$\chi = \phi_1 - \phi_2, \quad \phi = \phi_1 + \phi_2, \quad (2.9)$$

where  $-2\pi \leq \chi \leq 2\pi$  and  $0 \leq \phi \leq 4\pi$  for a fixed  $\chi$ . It should be noted that (i) the azimuthal angle difference,  $\chi$ , is independent of the final state, while the azimuthal angle sum,  $\phi$ , depends on the scattering plane, and (ii) both angles are invariant with respect to the Lorentz boost along the two-photon beam direction.

It is now straightforward to obtain the angular dependence of the  $\gamma\gamma \rightarrow X$  cross section on the initial beam polarizations

$$\begin{aligned} \Sigma(\xi, \bar{\xi}; \eta, \bar{\eta}; \chi, \phi) &\equiv \sum_X | \langle X|M|\xi, \bar{\xi}; \eta, \bar{\eta}; \chi, \phi \rangle |^2 \\ &= \frac{1}{4} \sum_X \left[ |M_{++}|^2 + |M_{+-}|^2 + |M_{-+}|^2 + |M_{--}|^2 \right] \\ &\quad + \frac{\xi}{4} \sum_X \left[ |M_{++}|^2 + |M_{+-}|^2 - |M_{-+}|^2 - |M_{--}|^2 \right] \\ &\quad + \frac{\bar{\xi}}{4} \sum_X \left[ |M_{++}|^2 - |M_{+-}|^2 + |M_{-+}|^2 - |M_{--}|^2 \right] \end{aligned}$$

$$\begin{aligned}
& + \frac{\xi \bar{\xi}}{4} \sum_X \left[ |M_{++}|^2 - |M_{+-}|^2 - |M_{-+}|^2 + |M_{--}|^2 \right] \\
& - \frac{\eta}{2} \text{Re} \left[ e^{-i(\chi+\phi)} \sum_X \left( M_{++} M_{-+}^* + M_{+-} M_{--}^* \right) \right] \\
& - \frac{\bar{\eta}}{2} \text{Re} \left[ e^{-i(\chi-\phi)} \sum_X \left( M_{++} M_{+-}^* + M_{-+} M_{--}^* \right) \right] \\
& - \frac{\eta \bar{\xi}}{2} \text{Re} \left[ e^{-i(\chi+\phi)} \sum_X \left( M_{++} M_{-+}^* - M_{+-} M_{--}^* \right) \right] \\
& - \frac{\bar{\eta} \xi}{2} \text{Re} \left[ e^{-i(\chi-\phi)} \sum_X \left( M_{++} M_{+-}^* - M_{-+} M_{--}^* \right) \right] \\
& + \frac{\eta \bar{\eta}}{2} \text{Re} \left[ e^{-2i\phi} \sum_X \left( M_{+-} M_{-+}^* \right) + e^{-2i\chi} \sum_X \left( M_{++} M_{--}^* \right) \right], \quad (2.10)
\end{aligned}$$

where the summation over  $X$  is for the polarizations of the final states, and  $(\xi, \bar{\xi})$  denote the degrees of circular polarization and  $(\eta, \bar{\eta})$  denote those of linear polarization of the two initial photon beams, respectively. They are expressed in terms of two parameters  $\alpha_1$  and  $\alpha_2$  by

$$\begin{aligned}
\xi &= P \cos(2\alpha_1), & \bar{\xi} &= \bar{P} \cos(2\alpha_2), \\
\eta &= P \sin(2\alpha_1), & \bar{\eta} &= \bar{P} \sin(2\alpha_2), \quad (2.11)
\end{aligned}$$

where  $P$  and  $\bar{P}$  ( $0 \leq P, \bar{P} \leq 1$ ) are the polarization degrees of the two colliding photons.

It is easy to check that there are sixteen independent terms, which are all measurable in polarized two-photon collisions. We find that purely linearly polarized photon beams allow us to determine nine terms among all the sixteen terms, while purely circularly polarized photon beams allow us to determine only four terms. The first term in Eq. (2.10), which corresponds to the unpolarized cross section, is determined in both cases. However, both circular and linear polarizations are needed to determine the remaining four terms.

Even though we obtain more information with both circularly and linearly polarized beams, we study in this paper mainly the case where two photons are linearly polarized but not circularly polarized. The expression of the angular dependence then greatly simplifies to

$$\mathcal{D}(\eta, \bar{\eta}; \chi, \phi) = \Sigma_{\text{unpol}} - \frac{1}{2} \text{Re} \left[ \left( \eta e^{-i\phi} + \bar{\eta} e^{i\phi} \right) e^{-i\chi} \Sigma_{02} \right]$$



$$\begin{aligned}
& + \frac{1}{2} \text{Re} \left[ \left( \eta e^{-i\phi} - \bar{\eta} e^{i\phi} \right) e^{-i\chi} \Delta_{02} \right] + \eta \bar{\eta} \text{Re} \left[ e^{-2i\phi} \Sigma_{22} + e^{-2i\chi} \Sigma_{00} \right], \quad (2.12a) \\
& = \Sigma_{\text{unpol}} - \frac{1}{2} [\eta \cos(\phi + \chi) + \bar{\eta} \cos(\phi - \chi)] \mathcal{R}(\Sigma_{02}) \\
& \quad + \frac{1}{2} [\eta \sin(\phi + \chi) - \bar{\eta} \sin(\phi - \chi)] \mathcal{I}(\Sigma_{02}) \\
& \quad - \frac{1}{2} [\eta \cos(\phi + \chi) - \bar{\eta} \cos(\phi - \chi)] \mathcal{R}(\Delta_{02}) \\
& \quad + \frac{1}{2} [\eta \sin(\phi + \chi) + \bar{\eta} \sin(\phi - \chi)] \mathcal{I}(\Delta_{02}) \\
& \quad + \eta \bar{\eta} \cos(2\phi) \mathcal{R}(\Sigma_{22}) + \eta \bar{\eta} \sin(2\phi) \mathcal{I}(\Sigma_{22}) \\
& \quad + \eta \bar{\eta} \cos(2\chi) \mathcal{R}(\Sigma_{00}) + \eta \bar{\eta} \sin(2\chi) \mathcal{I}(\Sigma_{00}), \quad (2.12b)
\end{aligned}$$

where the invariant functions are defined as

$$\begin{aligned}
\Sigma_{\text{unpol}} &= \frac{1}{4} \sum_X \left[ |M_{++}|^2 + |M_{+-}|^2 + |M_{-+}|^2 + |M_{--}|^2 \right] \\
\Sigma_{02} &= \frac{1}{2} \sum_X \left[ M_{++}(M_{+-}^* + M_{-+}^*) + (M_{+-} + M_{-+})M_{--}^* \right] \\
\Delta_{02} &= \frac{1}{2} \sum_X \left[ M_{++}(M_{+-}^* - M_{-+}^*) - (M_{+-} - M_{-+})M_{--}^* \right] \\
\Sigma_{22} &= \frac{1}{2} \sum_X (M_{+-}M_{-+}^*), \quad \Sigma_{00} = \frac{1}{2} \sum_X (M_{++}M_{--}^*), \quad (2.13)
\end{aligned}$$

with the subscripts, 0 and 2, representing the magnitude of the sum of the helicities of the initial two-photon system.

## B. Symmetry properties

It is useful to classify the invariant functions according to their transformation properties under the discrete symmetries, CP and  $\text{CPT}\tilde{} [11]$ . We find that CP invariance leads to the relations

$$\sum_X \left( M_{\lambda_1 \lambda_2} M_{\lambda'_1 \lambda'_2}^* \right) = \sum_X \left( M_{-\lambda_2, -\lambda_1} M_{-\lambda'_2, -\lambda'_1}^* \right), \quad (2.14a)$$

$$d\sigma(\phi, \chi; \eta, \bar{\eta}) = d\sigma(\phi, -\chi; \bar{\eta}, \eta), \quad (2.14b)$$

and, if there are no absorptive parts in the amplitudes,  $\text{CP}\tilde{} [11]$  invariance leads to the relations

$$\sum_X \left( M_{\lambda_1 \lambda_2} M_{\lambda'_1 \lambda'_2}^* \right) = \sum_X \left( M_{-\lambda_2, -\lambda_1}^* M_{-\lambda'_2, -\lambda'_1} \right), \quad (2.15a)$$

$$d\sigma(\phi, \chi; \eta, \bar{\eta}) = d\sigma(-\phi, \chi; \bar{\eta}, \eta). \quad (2.15b)$$

The nine invariant functions in Eq. (2.12b) can then be divided into four categories under CP and CPT: even-even, even-odd, odd-even, and odd-odd terms as in Table 1. CP-odd coefficients directly measure CP violation and CPT-odd terms indicate rescattering effects (absorptive parts in the scattering amplitudes). Table 1 shows that there exist three CP-odd functions;  $\mathcal{I}(\Sigma_{02})$ ,  $\mathcal{I}(\Sigma_{00})$  and  $\mathcal{R}(\Delta_{02})$ . Here,  $\mathcal{R}$  and  $\mathcal{I}$  are for real and imaginary parts, respectively. While the first two terms are CPT-even, the last term  $\mathcal{R}(\Delta_{02})$  is CPT-odd. Since the CPT-odd term  $\mathcal{R}(\Delta_{02})$  requires the absorptive part in the amplitude, it is generally expected to be smaller in magnitude than the CPT-even terms. We therefore study the two CP-odd and CPT-even distributions;  $\mathcal{I}(\Sigma_{02})$  and  $\mathcal{I}(\Sigma_{00})$ .

TABLE I. CP and CPT properties of the invariant functions and the angular distributions.

CP	CPT	Invariant functions	Angular dependences
even	even	$\Sigma_{\text{unpol}}$	
		$\mathcal{R}(\Sigma_{02})$	$\eta \cos(\phi + \chi) + \bar{\eta} \cos(\phi - \chi)$
		$\mathcal{R}(\Sigma_{22})$	$\eta \bar{\eta} \cos(2\phi)$
		$\mathcal{R}(\Sigma_{00})$	$\eta \bar{\eta} \cos(2\chi)$
even	odd	$\mathcal{I}(\Delta_{02})$	$\eta \sin(\phi + \chi) + \bar{\eta} \sin(\phi - \chi)$
		$\mathcal{I}(\Sigma_{22})$	$\eta \bar{\eta} \sin(2\phi)$
odd	even	$\mathcal{I}(\Sigma_{02})$	$\eta \sin(\phi + \chi) - \bar{\eta} \sin(\phi - \chi)$
		$\mathcal{I}(\Sigma_{00})$	$\eta \bar{\eta} \sin(2\chi)$
odd	odd	$\mathcal{R}(\Delta_{02})$	$\eta \cos(\phi + \chi) - \bar{\eta} \cos(\phi - \chi)$

We can define two CP-odd asymmetries from the two distributions,  $\mathcal{I}(\Sigma_{02})$  and  $\mathcal{I}(\Sigma_{00})$ . First, we note that the  $\Sigma_{00}$  term does not depend on the azimuthal angle  $\phi$  whereas the  $\Sigma_{02}$  does. In order to improve the observability we may integrate the  $\mathcal{I}(\Sigma_{02})$  term over the

azimuthal angle  $\phi$  with an appropriate weight function. Without any loss of generality we can take  $\eta = \bar{\eta}$ . Then, the quantity  $\mathcal{I}(\Sigma_{00})$  in Eq. (2.12b) can be separated by taking the difference of the distributions at  $\chi = \pm\pi/4$  and the  $\mathcal{I}(\Sigma_{02})$  by taking the difference of the distributions at  $\chi = \pm\pi/2$ . As a result we obtain the following two integrated CP-odd asymmetries:

$$\hat{A}_{02} = \left(\frac{2}{\pi}\right) \frac{\mathcal{I}(\Sigma_{02})}{\Sigma_{\text{unpol}}}, \quad \hat{A}_{00} = \frac{\mathcal{I}(\Sigma_{00})}{\Sigma_{\text{unpol}}}, \quad (2.16)$$

where the factor  $(2/\pi)$  in the  $\hat{A}_{02}$  stems from taking the average over the azimuthal angle  $\phi$  with the weight function  $\text{sign}(\cos \phi)$ :

$$\hat{A}_{02} = \frac{\int_0^{4\pi} d\phi [\text{sign}(\cos \phi)] \left[ \left(\frac{d\sigma}{d\phi}\right)_{\chi=\frac{\pi}{2}} - \left(\frac{d\sigma}{d\phi}\right)_{\chi=-\frac{\pi}{2}} \right]}{\int_0^{4\pi} d\phi \left[ \left(\frac{d\sigma}{d\phi}\right)_{\chi=\frac{\pi}{2}} + \left(\frac{d\sigma}{d\phi}\right)_{\chi=-\frac{\pi}{2}} \right]}, \quad (2.17a)$$

$$\hat{A}_{00} = \frac{\int_0^{4\pi} d\phi \left[ \left(\frac{d\sigma}{d\phi}\right)_{\chi=\frac{\pi}{4}} - \left(\frac{d\sigma}{d\phi}\right)_{\chi=-\frac{\pi}{4}} \right]}{\int_0^{4\pi} d\phi \left[ \left(\frac{d\sigma}{d\phi}\right)_{\chi=\frac{\pi}{4}} + \left(\frac{d\sigma}{d\phi}\right)_{\chi=-\frac{\pi}{4}} \right]}. \quad (2.17b)$$

In pair production processes such as  $\gamma\gamma \rightarrow W^+W^-$ , all the distributions,  $\Sigma_i$ , can be integrated over the scattering angle  $\theta$  with a CP-even angular cut so as to test CP violation.

### III. PHOTON LINEAR COLLIDER

In this section we give a short review of the powerful mechanism of providing an energetic, highly polarized photon beam; the Compton laser backscattering [14] off energetic electron or positron beams. After the review we introduce two functions to describe partial linear polarization transfer from the laser beams to the backscattered photon beams for the photon-photon collisions.

We assume that the electron or positron beams are unpolarized and the laser beams are purely linearly polarized. Even in that case the backscattered photon beam is not purely linearly polarized but only part of the laser linear polarization is transferred to the backscattered energetic high-energy photon beam.

## A. Photon spectrum

We consider the situation where a purely linearly polarized laser beam of frequency  $\omega_0$  is focused upon an unpolarized electron or positron beam of energy  $E$ . In the collision of a laser photon beam and a linac electron beam, a high energy photon beam of energy  $\omega$ , which is partially linearly polarized, is emitted at a very small angle, along with the scattered electron beam of energy  $E' = E - \omega$ . The kinematics of the Compton backscattering process is then characterized by the dimensionless parameters  $x$  and  $y$ :

$$x = \frac{4E\omega_0}{m_e^2} \approx 15.3 \left( \frac{E}{\text{TeV}} \right) \left( \frac{\omega_0}{\text{eV}} \right), \quad y = \frac{\omega}{E}. \quad (3.1)$$

In general, the backscattered photon energies increase with  $x$ ; the maximum photon energy fraction is given by  $y_m = x/(1+x)$ . Operation below the threshold [14] for  $e^+e^-$  pair production in collisions between the laser beam and the Compton-backscattered photon beam requires  $x \leq 2(1 + \sqrt{2}) \approx 4.83$ ; the lower bound on  $x$  depends on the lowest available laser frequency and the production threshold of a given final state.

The backscattered photon energy spectrum is given by the function

$$\phi_0(y) = \frac{1}{1-y} + 1 - y - 4r(1-r), \quad (3.2)$$

where  $r = y/(x(1-y))$ . Fig.2(a) shows the photon energy spectrum for various values of  $x$ . Clearly large values of  $x$  are favored to produce highly energetic photons. On the other hand, the degree of linear polarization of the backscattered photon beam is given by [14]

$$\eta(y) = \frac{2r^2}{\phi_0(y)}. \quad (3.3)$$

The maximum linear polarization is reached for  $y = y_m$  (See Fig. 2(b)),

$$\eta_{\max} = \eta(y_m) = \frac{2(1+x)}{1+(1+x)^2}, \quad (3.4)$$

and approaches unity for small values of  $x$ . In order to retain large linear polarization we should keep the  $x$  value as small as possible.

## B. Linear polarization transfers

In the two-photon collision case only part of each laser linear polarization is transferred to the high-energy photon beam. We introduce two functions,  $\mathcal{A}_\eta$  and  $\mathcal{A}_{\eta\eta}$ , to denote the degrees of linear polarization transfer [19] as

$$\mathcal{A}_\eta(\tau) = \frac{\langle \phi_0 \phi_3 \rangle_\tau}{\langle \phi_0 \phi_0 \rangle_\tau}, \quad \mathcal{A}_{\eta\eta}(\tau) = \frac{\langle \phi_3 \phi_3 \rangle_\tau}{\langle \phi_0 \phi_0 \rangle_\tau}, \quad (3.5)$$

where  $\phi_3(y) = 2r^2$  and  $\tau$  is the ratio of the  $\gamma\gamma$  c.m. energy squared  $\hat{s}$  to the  $e^+e^-$  collider energy squared  $s$ . The function  $\mathcal{A}_\eta$  is for the collision of an unpolarized photon beam and a linearly polarized photon beam and the function  $\mathcal{A}_{\eta\eta}$  for the collision of two linearly polarized photon beams. The convolution integrals  $\langle \phi_i \phi_j \rangle_\tau$  ( $i, j = 0, 3$ ) for a fixed value of  $\tau$  are defined as

$$\langle \phi_i \phi_j \rangle_\tau = \frac{1}{\mathcal{N}^2(x)} \int_{\tau/y_m}^{y_m} \frac{dy}{y} \phi_i(y) \phi_j(\tau/y), \quad (3.6)$$

where the normalization factor  $\mathcal{N}(x)$  is given by the integral of the photon energy spectrum  $\phi_0$  over  $y$  as

$$\mathcal{N}(x) = \int_0^{y_m} \phi_0(y) dy = \ln(1+x) \left[ 1 - \frac{4}{x} - \frac{8}{x^2} \right] + \frac{1}{2} + \frac{8}{x} - \frac{1}{2(1+x)^2}. \quad (3.7)$$

The event rates of the  $\gamma\gamma \rightarrow X$  reaction with polarized photons can be obtained by folding a photon luminosity spectral function with the  $\gamma\gamma \rightarrow X$  production cross section as (for  $\eta = \bar{\eta}$ )

$$dN_{\gamma\gamma \rightarrow X} = dL_{\gamma\gamma} \cdot d\hat{\sigma}(\gamma\gamma \rightarrow X), \quad (3.8)$$

where

$$dL_{\gamma\gamma} = \kappa^2 L_{ee} \langle \phi_0 \phi_0 \rangle_\tau d\tau, \quad (3.9a)$$

$$d\hat{\sigma}(\gamma\gamma \rightarrow X) = \frac{1}{2\hat{s}} d\Phi_X \left[ \Sigma_{\text{unpol}} - \eta \mathcal{A}_\eta \cos \phi \text{Re} \left( e^{-i\chi} \Sigma_{02} \right) \right. \\ \left. + \eta \mathcal{A}_\eta \sin \phi \text{Im} \left( e^{-i\chi} \Delta_{02} \right) + \eta^2 \mathcal{A}_{\eta\eta} \text{Re} \left( e^{-2i\phi} \Sigma_{22} + e^{-2i\chi} \Sigma_{00} \right) \right]. \quad (3.9b)$$

Here,  $\kappa$  is the  $e\text{-}\gamma$  conversion coefficient in the Compton backscattering and  $d\Phi_X$  is the phase space factor of the final state, which is given for  $X = W^+W^-$  by

$$d\Phi_{W^+W^-} = \frac{\hat{\beta}}{32\pi^2} d\cos\hat{\theta} d\phi. \quad (3.10)$$

The distribution (3.9b) of event rates enables us to construct two CP-odd asymmetries;

$$A_{02} = \left(\frac{2}{\pi}\right) \frac{N_{02}}{N_{\text{unpol}}}, \quad A_{00} = \frac{N_{00}}{N_{\text{unpol}}}, \quad (3.11)$$

where with  $\tau_{\text{max}} = y_m^2$  and  $\tau_{\text{min}} = M_X^2/s$  we have for the event distributions

$$\begin{pmatrix} N_{\text{upl}} \\ N_{02} \\ N_{00} \end{pmatrix} = \kappa^2 L_{ee} \frac{1}{2s} \int_{\tau_{\text{min}}}^{\tau_{\text{max}}} \frac{d\tau}{\tau} \int d\Phi_X \langle \phi_0 \phi_0 \rangle_\tau \begin{pmatrix} \Sigma_{\text{unpol}} \\ \eta \mathcal{A}_\eta \mathcal{I}(\Sigma_{02}) \\ \eta^2 \mathcal{A}_{\eta\eta} \mathcal{I}(\Sigma_{00}) \end{pmatrix}. \quad (3.12)$$

The asymmetries depend crucially on the two-photon spectrum and the two linear polarization transfers.

We first investigate the  $\sqrt{\tau}$  dependence of the two-photon spectrum and the two linear polarization transfers,  $A_\eta$  and  $A_{\eta\eta}$  by varying the value of the dimensionless parameter  $x$ . Three values of  $x$  are chosen;  $x = 0.5, 1$ , and  $4.83$ . Two figures in Fig. 3 clearly show that the energy of two photons reaches higher ends for larger  $x$  values but the maximum linear polarization transfers are larger for smaller  $x$  values. We also note that  $A_\eta$  (solid lines) is larger than  $A_{\eta\eta}$  (dashed lines) in the whole range of  $\sqrt{\tau}$ . We should keep the parameter  $x$  as large as possible to reach higher energies. However, larger CP-odd asymmetries can be obtained for smaller  $x$  values. Therefore, there should exist a compromised value of  $x$  for the optimal observability of CP violation. The energy dependence of the subprocess cross section and that of the CP-odd asymmetries are both essential to find the optimal  $x$  value.

#### IV. CP-ODD WEAK-BOSON COUPLINGS

In this section we describe how CP violation from new interactions among electroweak vector bosons can be probed in a model-independent way in the  $W$  pair production in two-

photon collisions. We adopt the effective Lagrangian with most general CP-odd interactions among electroweak gauge bosons. The basic assumptions are that the operators with lowest energy dimension (6) dominate the CP-odd amplitudes and that they respect the electroweak gauge invariance which is broken spontaneously by an effective SU(2)-doublet scalar. The effective Lagrangian then determines the energy dependence of the scattering amplitudes at energies below the new physics scale.

### A. Effective Lagrangian with CP-odd operators

The effects of new physics are parametrized by using an effective Lagrangian in a model and process independent way. As for the electroweak gauge symmetry breaking parameter, we adopt the effective SU(2)-doublet scalar field  $\Phi$ , which is more convenient when a physical Higgs boson appears at low energies. In addition to the Higgs doublet field  $\Phi$ , the building blocks of the gauge-invariant operators are the covariant derivatives of the Higgs field,  $D_\mu \Phi$ , and the non-Abelian-field strength tensors  $W_{\mu\nu}^I$  ( $I = 1, 2, 3$ ) and  $B_{\mu\nu}$  of the SU(2)<sub>L</sub> and U(1)<sub>Y</sub> gauge fields, respectively. Considering CP-odd interactions of dimension six, we can construct six independent operators that are relevant for the process  $\gamma\gamma \rightarrow W^+W^-$

$$\mathcal{O}_{B\tilde{B}} = g'^2(\Phi^\dagger\Phi)B_{\mu\nu}\tilde{B}^{\mu\nu}, \quad (4.1a)$$

$$\mathcal{O}_{B\tilde{W}} = gg'(\Phi^\dagger\sigma^I\Phi)B_{\mu\nu}\tilde{W}^{I\mu\nu}, \quad (4.1b)$$

$$\mathcal{O}_{W\tilde{W}} = g^2(\Phi^\dagger\Phi)W_{\mu\nu}^I\tilde{W}^{I\mu\nu}, \quad (4.1c)$$

$$\mathcal{O}_{\tilde{B}} = ig'[(D_\mu\Phi)^\dagger(D_\nu\Phi)]\tilde{B}^{\mu\nu}, \quad (4.1d)$$

$$\mathcal{O}_{\tilde{W}} = ig[(D_\mu\Phi)^\dagger\sigma^I(D_\nu\Phi)]\tilde{W}^{I\mu\nu}, \quad (4.1e)$$

$$\mathcal{O}_{WW\tilde{W}} = g^3\epsilon^{IJK}\tilde{W}^{I\mu\nu}W_\nu^{J\rho}W_{\rho\mu}^K, \quad (4.1f)$$

where  $\tilde{W}^{I\mu\nu} = \frac{1}{2}\epsilon^{\mu\nu\alpha\beta}W_{\alpha\beta}^I$ ,  $\tilde{B}^{\mu\nu} = \frac{1}{2}\epsilon^{\mu\nu\alpha\beta}\tilde{B}_{\alpha\beta}$ ,  $\sigma^I$  are the Pauli matrices, and the SU(2)<sub>L</sub>×U(1)<sub>Y</sub> covariant derivative is given by

$$D_\mu = \partial_\mu + ig\frac{\sigma^I}{2}W_\mu^I + ig'YB_\mu, \quad (4.2)$$

with the isospin indices  $I, J$  and  $K$  ( $= 1, 2, 3$ ) and the SU(2) and U(1) couplings,  $g$  and  $g'$ , respectively. The effective Lagrangian is written as

$$\mathcal{L} = \mathcal{L}_{SM} + \frac{1}{\Lambda^2} \left[ f_{B\tilde{B}} \mathcal{O}_{B\tilde{B}} + f_{B\tilde{W}} \mathcal{O}_{B\tilde{W}} + f_{W\tilde{W}} \mathcal{O}_{W\tilde{W}} + f_{\tilde{B}} \mathcal{O}_{\tilde{B}} + f_{\tilde{W}} \mathcal{O}_{\tilde{W}} + f_{WW\tilde{W}} \mathcal{O}_{WW\tilde{W}} \right], \quad (4.3)$$

where the dimension-six terms  $\mathcal{O}_i$  are scaled by the common dimensional parameter  $\Lambda$  with dimensionless coefficients  $f_i$ . The fields  $W^3$  and  $B$  are related in terms of the Weinberg angle  $\theta_W$  to the  $Z$  and photon fields,  $Z$  and  $A$  as

$$\begin{pmatrix} W^3 \\ B \end{pmatrix} = \begin{pmatrix} \cos \theta_W & \sin \theta_W \\ -\sin \theta_W & \cos \theta_W \end{pmatrix} \begin{pmatrix} Z \\ A \end{pmatrix}. \quad (4.4)$$

Incidentally, as we are interested in the photon-induced process  $\gamma\gamma \rightarrow W^+W^-$ , we can neglect the terms involving the  $Z$  field. Then all the terms for the process  $\gamma\gamma \rightarrow W^+W^-$  can be derived by the following effective replacements

$$W_{\mu\nu}^- \rightarrow (\partial_\mu - ieA_\nu)W_\nu^- - (\partial_\nu - ieA_\mu)W_\mu^-, \quad (4.5a)$$

$$W_{\mu\nu}^+ \rightarrow (\partial_\mu + ieA_\nu)W_\nu^+ - (\partial_\nu + ieA_\mu)W_\mu^+, \quad (4.5b)$$

$$W_{\mu\nu}^3 \rightarrow \sin \theta_W F_{\mu\nu} + \frac{ie}{\sin \theta_W} (W_\mu^+ W_\nu^- - W_\nu^+ W_\mu^-), \quad (4.5c)$$

$$B_{\mu\nu} \rightarrow \cos \theta_W F_{\mu\nu}, \quad (4.5d)$$

where  $F_{\mu\nu} = \partial_\mu A_\nu - \partial_\nu A_\mu$ . We take the unitary gauge where the scalar doublet  $\Phi$  with hypercharge  $Y = \frac{1}{2}$  takes the form

$$\Phi = \frac{1}{\sqrt{2}}(v + H) \begin{bmatrix} 0 \\ 1 \end{bmatrix}. \quad (4.6)$$

$H$  denotes the Higgs boson in the SM. It is now straightforward to obtain the new CP-odd vertices among terms of the component fields,  $W^\pm$ ,  $A$ , and  $H$  in the unitary gauge.



## B. CP-odd vertices

In this section we give the Feynman rules for the  $\gamma WW$ ,  $\gamma\gamma H$ ,  $HWW$ , and  $\gamma\gamma WW$  vertices, relevant for the  $\gamma\gamma \rightarrow W^+W^-$  reaction. Table 2 shows which vertices already exist in the SM at tree level and which new vertices appear from the new dimension-six CP-odd operators. Firstly, the three operators,  $\mathcal{O}_{B\tilde{B}}$ ,  $\mathcal{O}_{B\tilde{W}}$ , and  $\mathcal{O}_{W\tilde{W}}$  contribute to the  $\gamma\gamma H$  vertex. Secondly, we find that the operator  $\mathcal{O}_{WW\tilde{W}}$  gives a new CP-odd  $\gamma WW$  vertex and a new CP-odd  $\gamma\gamma WW$  vertex, which are related by U(1) electromagnetic gauge invariance. In addition, the three operators,  $\mathcal{O}_{B\tilde{W}}$ ,  $\mathcal{O}_{\tilde{W}}$ , and  $\mathcal{O}_{\tilde{B}}$  contribute to the  $\gamma WW$  vertex as well. Thirdly, we find that  $\mathcal{O}_{W\tilde{W}}$  and  $\mathcal{O}_{\tilde{W}}$  contribute to the  $HWW$  vertex.

TABLE II. Vertices relevant for the process  $\gamma\gamma \rightarrow W^+W^-$  in the SM with dimension-six CP-odd terms.

Vertex	$\gamma WW$	$\gamma\gamma WW$	$HWW$	$\gamma\gamma H$
SM	○	○	○	X
$\mathcal{O}_{B\tilde{B}}$	X	X	X	○
$\mathcal{O}_{B\tilde{W}}$	○	X	X	○
$\mathcal{O}_{W\tilde{W}}$	X	X	○	○
$\mathcal{O}_{\tilde{B}}$	○	X	X	X
$\mathcal{O}_{\tilde{W}}$	○	X	○	X
$\mathcal{O}_{WW\tilde{W}}$	○	○	X	X

For convenience we define four new dimensionless form factors,  $Y_i$  ( $i = 1$  to 4), which are related with the coefficients,  $f_i$ 's ( $i = B\tilde{B}, B\tilde{W}, W\tilde{W}, \tilde{B}, \tilde{W}, WW\tilde{W}$ ) as

$$\begin{aligned}
Y_1 &= \left(\frac{m_W}{\Lambda}\right)^2 \left[ f_{B\tilde{W}} + \frac{1}{4}f_{\tilde{B}} + f_{\tilde{W}} \right], & Y_2 &= \left(\frac{m_W}{\Lambda}\right)^2 \frac{g^2}{4} f_{WW\tilde{W}}, \\
Y_3 &= \left(\frac{m_W}{\Lambda}\right)^2 \left[ f_{W\tilde{W}} + \frac{1}{4}f_{\tilde{W}} \right], & Y_4 &= \left(\frac{m_W}{\Lambda}\right)^2 \left[ f_{B\tilde{B}} - f_{B\tilde{W}} - f_{W\tilde{W}} \right].
\end{aligned} \tag{4.7}$$

If all the coefficients,  $f_i$ , are of the similar size, then  $Y_2$  would be about ten times smaller than the other form factors in size because of the factor  $g^2/4 \sim 0.1$ . We denote the Feynman

rule of a vertex  $V$  in the form;  $ie\Gamma_V$ . It is then straightforward to derive the explicit form of two simple  $\gamma\gamma H$  and  $HWW$  vertices;

$$\Gamma_{\gamma\gamma H}^{\mu\nu}(k_1, k_2) = \frac{8Y_4}{m_W} \sin\theta_W \epsilon^{\mu\nu\rho\sigma} k_{1\rho} k_{2\sigma}, \quad (4.8)$$

$$\Gamma_{HWW}^{\alpha\beta}(q_1, q_2) = \frac{m_W}{\sin\theta_W} g^{\alpha\beta} + \frac{8Y_3}{m_W \sin\theta_W} \epsilon^{\alpha\beta\rho\sigma} q_{1\rho} q_{2\sigma}, \quad (4.9)$$

where  $k_1(\mu)$  and  $k_2(\nu)$  are four-momenta (Lorentz indices) of two incoming photons and  $q_1(\alpha)$  and  $q_2(\beta)$  are four-momenta (Lorentz indices) for the outgoing  $W^+$  and  $W^-$ , respectively. In the SM the  $\gamma\gamma H$  vertex appears in the one-loop level, we do not study its consequences in this paper. The triple  $\gamma WW$  vertex is

$$\begin{aligned} \Gamma_{\gamma WW}^{\mu\alpha\beta}(k, q_1, q_2) &= (q_1 - q_2)^\mu g^{\alpha\beta} - (q_1 + k)^\beta g^{\mu\alpha} + (k + q_2)^\alpha g^{\mu\beta} \\ &\quad - 4Y_1 \epsilon^{\mu\alpha\beta\rho} k_\rho \\ &\quad + 12 \frac{Y_2}{m_W^2} \left[ 2(q_1 \cdot q_2) \epsilon^{\mu\alpha\beta\rho} - q_2^\alpha \epsilon^{\mu\beta\rho\sigma} (q_1 - q_2)_\sigma - q_1^\beta \epsilon^{\mu\alpha\rho\sigma} (q_1 - q_2)_\sigma \right] k_\rho, \end{aligned} \quad (4.10)$$

where  $k = q_1 + q_2$ , and the quartic  $\gamma\gamma WW$  vertex is

$$\begin{aligned} \Gamma_{\gamma\gamma WW}^{\mu\nu\alpha\beta}(k_1, k_2, q_1, q_2) &= -2g^{\mu\nu} g^{\alpha\beta} + g^{\mu\alpha} g^{\nu\beta} + g^{\mu\beta} g^{\nu\alpha} \\ &\quad + 8 \frac{Y_2}{m_W^2} \left[ 2g^{\alpha\beta} \epsilon^{\mu\nu\rho\sigma} k_{1\rho} k_{2\sigma} + 2g^{\mu\nu} \epsilon^{\alpha\beta\rho\sigma} q_{1\rho} q_{2\sigma} \right. \\ &\quad - g^{\mu\alpha} \epsilon^{\nu\beta\rho\sigma} q_{2\rho} k_{2\sigma} - g^{\mu\beta} \epsilon^{\nu\alpha\rho\sigma} q_{1\rho} k_{2\sigma} \\ &\quad - g^{\nu\alpha} \epsilon^{\mu\beta\rho\sigma} q_{2\rho} k_{1\sigma} - g^{\nu\beta} \epsilon^{\mu\alpha\rho\sigma} q_{1\rho} k_{1\sigma} + (k_1 - k_2) \cdot (q_1 - q_2) \epsilon^{\mu\nu\alpha\beta} \\ &\quad + k_2^\mu \epsilon^{\nu\alpha\beta\rho} (q_1 - q_2)_\rho + k_1^\nu \epsilon^{\mu\alpha\beta\rho} (q_1 - q_2)_\rho \\ &\quad + q_2^\alpha \epsilon^{\mu\nu\beta\rho} (k_1 - k_2)_\rho + q_1^\beta \epsilon^{\mu\nu\alpha\rho} (k_1 - k_2)_\rho \\ &\quad + (q_1 - q_2)^\mu \epsilon^{\nu\alpha\beta\rho} (k_1 + k_2)_\rho + (q_1 - q_2)^\nu \epsilon^{\mu\alpha\beta\rho} (k_1 + k_2)_\rho \\ &\quad \left. + (k_1 - k_2)^\alpha \epsilon^{\mu\nu\beta\rho} (q_1 + q_2)_\rho + (k_1 - k_2)^\beta \epsilon^{\mu\nu\alpha\rho} (q_1 + q_2)_\rho \right]. \end{aligned} \quad (4.11)$$

## V. HELICITY AMPLITUDES FOR $\gamma\gamma \rightarrow W^+ W^-$

In this section we present the complete calculation of polarization amplitudes for the process

$$\gamma(k_1, \lambda_1) + \gamma(k_2, \lambda_2) \rightarrow W^+(q_1, \lambda_3) + W^-(q_2, \lambda_4), \quad (5.1)$$

with the effective Lagrangian (4.3) in Section IV. The four-momentum and the helicity of each particle are shown in the parenthesis. The helicities of the  $W$  are given in the  $\gamma\gamma$  c.m. frame. Helicity amplitudes contain full information of the process. The relative phases of the amplitudes are essential because the interference of different photon and  $W$  helicity states gives a nontrivial azimuthal-angle dependence.

By taking the two photon momenta along the  $z$ -axis and by taking the  $W^+$  momentum in the  $x$ - $z$  plane (see Fig. 1), the four-momenta are parametrized as

$$\begin{aligned} k_1^\mu &= \frac{\sqrt{\hat{s}}}{2}(1, 0, 0, 1), & k_2^\mu &= \frac{\sqrt{\hat{s}}}{2}(1, 0, 0, -1), \\ q_1^\mu &= \frac{\sqrt{\hat{s}}}{2}(1, \hat{\beta} \sin \theta, 0, \hat{\beta} \cos \theta), & q_2^\mu &= \frac{\sqrt{\hat{s}}}{2}(1, -\hat{\beta} \sin \theta, 0, -\hat{\beta} \cos \theta). \end{aligned} \quad (5.2)$$

The incoming photon polarization vectors are

$$\epsilon_1^\mu(\pm) = \mp \frac{1}{\sqrt{2}}(0, 1, \pm i, 0), \quad \epsilon_2^\mu(\pm) = \mp \frac{1}{\sqrt{2}}(0, 1, \mp i, 0), \quad (5.3)$$

and the transverse (helicity- $\pm 1$ ) and longitudinal (helicity-0) polarization vectors of the  $W^\pm$  bosons are

$$\begin{aligned} \epsilon_3^{*\mu}(\pm) &= \mp \frac{1}{\sqrt{2}}(0, \cos \theta, \mp i, -\sin \theta), & \epsilon_4^{*\mu}(\pm) &= \mp \frac{1}{\sqrt{2}}(0, -\cos \theta, \mp i, \sin \theta), \\ \epsilon_3^{*\mu}(0) &= \frac{\sqrt{\hat{s}}}{2m_W}(\hat{\beta}, \sin \theta, 0, \cos \theta), & \epsilon_4^{*\mu}(0) &= \frac{\sqrt{\hat{s}}}{2m_W}(\hat{\beta}, -\sin \theta, 0, -\cos \theta), \end{aligned} \quad (5.4)$$

respectively.

TABLE III. Explicit form of the  $d$  functions needed.

$d_{2,2}^2(\theta) = d_{-2,-2}^2(\theta) = \frac{1}{4}(1 + \cos \theta)^2$
$d_{2,-2}^2(\theta) = d_{-2,2}^2(\theta) = \frac{1}{4}(1 - \cos \theta)^2$
$d_{2,1}^2(\theta) = -d_{-2,-1}^2(\theta) = -\frac{1}{2}(1 + \cos \theta) \sin \theta$
$d_{2,-1}^2(\theta) = -d_{-2,1}^2(\theta) = \frac{1}{2}(1 - \cos \theta) \sin \theta$
$d_{2,0}^2(\theta) = d_{-2,0}^2(\theta) = d_{0,2}^2(\theta) = d_{0,-2}^2(\theta) = \sqrt{\frac{3}{8}} \sin^2 \theta$
$d_{0,1}^1(\theta) = d_{0,-1}^1(\theta) = \sqrt{\frac{1}{2}} \sin \theta$
$d_{0,0}^0(\theta) = 1$

The helicity amplitudes can then be parametrized as

$$\mathcal{M}_{\lambda_1\lambda_2;\lambda_3\lambda_4}(\theta) = e^2 \tilde{\mathcal{M}}_{\lambda_1\lambda_2;\lambda_3\lambda_4}(\theta) d_{\Delta\lambda_{12},\Delta\lambda_{34}}^{J_0}, \quad (5.5)$$

where  $\Delta\lambda_{12} = \lambda_1 - \lambda_2$ ,  $\Delta\lambda_{34} = \lambda_3 - \lambda_4$ ,  $J_0 = \max(|\Delta\lambda_{12}|, |\Delta\lambda_{34}|)$ , and  $d_{\Delta\lambda_{12},\Delta\lambda_{34}}^{J_0}$  is the  $d$  function. The explicit form of the  $d$  functions needed here is listed in Table 3.

We separate the amplitude into the SM contribution and the new CP-odd contributions with the factor  $i$  extracted

$$\tilde{\mathcal{M}} = \tilde{\mathcal{M}}_{SM} + i\tilde{\mathcal{M}}_N, \quad (5.6)$$

where the new contribution can be decomposed in the form

$$\tilde{\mathcal{M}}_N = Y_1 \tilde{\mathcal{M}}^{Y_1} + Y_2 \tilde{\mathcal{M}}^{Y_2} + Y_3 \tilde{\mathcal{M}}^{Y_3} + Y_4 \tilde{\mathcal{M}}^{Y_4}. \quad (5.7)$$

Here we retain only those terms with one insertion of CP-odd operators.

### A. The Standard Model amplitudes

The process  $\gamma\gamma \rightarrow W^+W^-$  is P and CP preserving in the SM at tree level. This leads to the following relations

$$\text{P : } \tilde{\mathcal{M}}_{\lambda_1\lambda_2;\lambda_3\lambda_4} = \tilde{\mathcal{M}}_{-\lambda_1,-\lambda_2;-\lambda_3,-\lambda_4}, \quad \text{CP : } \tilde{\mathcal{M}}_{\lambda_1\lambda_2;\lambda_3\lambda_4} = \tilde{\mathcal{M}}_{-\lambda_2,-\lambda_1;-\lambda_4,-\lambda_3}. \quad (5.8)$$

The Bose symmetry leads to the relation;

$$\tilde{\mathcal{M}}_{\lambda_1\lambda_2;\lambda_3\lambda_4} = \tilde{\mathcal{M}}_{\lambda_2\lambda_1;\lambda_3\lambda_4} \quad (\cos\theta \rightarrow -\cos\theta). \quad (5.9)$$

Let us rewrite the amplitude in the form

$$\tilde{\mathcal{M}}_{SM} = \frac{\tilde{\mathcal{N}}^{SM}}{1 - \hat{\beta}^2 \cos^2\theta}, \quad (5.10)$$

by extracting the  $t$ - and  $u$ -channel  $W$  boson propagator factor. It is clear that the coefficients  $\tilde{\mathcal{N}}$ 's satisfy the same P, CP and Bose-symmetry relations as  $\hat{\mathcal{M}}_{SM}$ . We find for the positive photon helicity ( $\lambda_1 = +$ ),

$$\begin{aligned}
\tilde{\mathcal{N}}_{++;++}^{SM} &= 2(1 + \hat{\beta})^2, & \tilde{\mathcal{N}}_{++;+0}^{SM} &= \tilde{\mathcal{N}}_{++;+-}^{SM} = \tilde{\mathcal{N}}_{++;0+}^{SM} = 0, \\
\tilde{\mathcal{N}}_{++;00}^{SM} &= -\frac{8}{\hat{r}}, & \tilde{\mathcal{N}}_{++;0-}^{SM} &= \tilde{\mathcal{N}}_{++;-+}^{SM} = \tilde{\mathcal{N}}_{++;-0}^{SM} = 0, \\
\tilde{\mathcal{N}}_{++;--}^{SM} &= 2(1 - \hat{\beta})^2, & \tilde{\mathcal{N}}_{+-;++}^{SM} &= \frac{32}{\sqrt{6}\hat{r}}, & \tilde{\mathcal{N}}_{+-;+-}^{SM} &= 8, \\
\tilde{\mathcal{N}}_{+-;+0}^{SM} &= \tilde{\mathcal{N}}_{+-;0+}^{SM} = \frac{8}{\sqrt{2}\hat{r}}, & \tilde{\mathcal{N}}_{+-;00}^{SM} &= 4\sqrt{\frac{2}{3}}(2 - \hat{\beta}^2),
\end{aligned} \tag{5.11}$$

where  $\hat{r} = \hat{s}/m_W^2$ . The other remaining coefficients can be obtained by using the P and CP relations (5.8) and the Bose-symmetry. We note the following three features of the SM amplitudes;

- The amplitudes for producing two  $W$ 's with the non-vanishing total spin component along the  $W$  boson momentum direction ( $\Delta\lambda_{34}$ ) vanish when the initial state has  $J_z = \Delta\lambda_{12} = 0$ .
- The amplitude for producing two longitudinal  $W$ 's from a  $J_z = 0$  initial state is suppressed by a factor of  $1/\hat{r}$  in the SM. The same behaviour should appear in the production of two charged scalars such as  $\gamma\gamma \rightarrow \pi^+\pi^-$ .
- The amplitudes for producing two right-(left-)handed  $W$ 's from two left-(right-)handed photons is suppressed by a factor of  $1/\hat{r}^2$ .

The results are consistent with those by Yehudai [3] and by Bélanger, *et.al* [8].

## B. CP-odd amplitudes

Every CP-odd amplitude and its CP-conjugate amplitude satisfies the following relation

$$\tilde{\mathcal{M}}_{\lambda_1\lambda_2;\lambda_3\lambda_4}^{Y_i} = -\tilde{\mathcal{M}}_{-\lambda_2,-\lambda_1;-\lambda_4,-\lambda_3}^{Y_i} \quad (i = 1, 2, 3, 4), \tag{5.12}$$

since the factor of  $i$  is extracted in the full helicity amplitude (5.6). It then follows that any CP self-conjugate amplitude has vanishing contribution from the CP-odd terms;

$$\tilde{\mathcal{M}}^{Y_i}(\pm\mp; \pm\mp) = \tilde{\mathcal{M}}^{Y_i}(\pm\mp; \mp\pm) = \tilde{\mathcal{M}}^{Y_i}(\pm\mp; 00) = 0 \quad (i = 1, 2, 3, 4). \tag{5.13}$$

The  $Y_1$  and  $Y_2$  terms contribute to the  $t$ - and  $u$ - channels and  $Y_2$  contributes to the contact  $\gamma\gamma WW$  diagram as well. By using the notation

$$\tilde{\mathcal{M}}^{Y_i} = \frac{\tilde{\mathcal{N}}^{Y_i}}{1 - \hat{\beta}^2 \cos^2 \theta}, \quad (i = 1, 2), \quad (5.14)$$

we find that the non-vanishing  $Y_1$  contributions are

$$\begin{aligned} \tilde{\mathcal{N}}_{++;++}^{Y_1} &= -\tilde{\mathcal{N}}_{--;--}^{Y_1} = 8 \left[ 2 + \hat{\beta}(1 + \cos^2 \theta) \right], \\ \tilde{\mathcal{N}}_{++;+0}^{Y_1} &= -\tilde{\mathcal{N}}_{--;0-}^{Y_1} = \tilde{\mathcal{N}}_{++;0+}^{Y_1} = -\tilde{\mathcal{N}}_{--;-0}^{Y_1} = 4\sqrt{\hat{r}}\hat{\beta}(1 + \hat{\beta}), \\ \tilde{\mathcal{N}}_{++;00}^{Y_1} &= -\tilde{\mathcal{N}}_{--;00}^{Y_1} = -4\hat{r}(1 - \hat{\beta}^2 \cos^2 \theta), \\ \tilde{\mathcal{N}}_{++;0-}^{Y_1} &= -\tilde{\mathcal{N}}_{--;+0}^{Y_1} = \tilde{\mathcal{N}}_{++;-0}^{Y_1} = -\tilde{\mathcal{N}}_{--;0+}^{Y_1} = -4\sqrt{\hat{r}}\hat{\beta}(1 - \hat{\beta}), \\ \tilde{\mathcal{N}}_{++;+-}^{Y_1} &= -\tilde{\mathcal{N}}_{--;+-}^{Y_1} = 8 \left[ 2 - \hat{\beta}(1 + \cos^2 \theta) \right], \\ \tilde{\mathcal{N}}_{+-;++}^{Y_1} &= -\tilde{\mathcal{N}}_{+-;--}^{Y_1} = \tilde{\mathcal{N}}_{-+;++}^{Y_1} = -\tilde{\mathcal{N}}_{-+;--}^{Y_1} = -\frac{32}{\sqrt{6}}\hat{\beta}, \\ \tilde{\mathcal{N}}_{+-;+0}^{Y_1} &= -\tilde{\mathcal{N}}_{+-;0-}^{Y_1} = \tilde{\mathcal{N}}_{-+;0+}^{Y_1} = -\tilde{\mathcal{N}}_{-+;-0}^{Y_1} = \tilde{\mathcal{N}}_{-+;+0}^{Y_1} \\ &= -\tilde{\mathcal{N}}_{-+;0-}^{Y_1} = \tilde{\mathcal{N}}_{-+;0+}^{Y_1} = -\tilde{\mathcal{N}}_{-+;-0}^{Y_1} = -4\sqrt{2\hat{r}}\hat{\beta}, \end{aligned} \quad (5.15)$$

and the non-vanishing  $Y_2$  contributions are

$$\begin{aligned} \tilde{\mathcal{N}}_{++;++}^{Y_2} &= -\tilde{\mathcal{N}}_{--;--}^{Y_2} = -12\hat{r} \left[ 1 - 3\hat{\beta} + \hat{\beta}^2 + \hat{\beta}^3 + (1 + \hat{\beta} - 3\hat{\beta}^2 + \hat{\beta}^3) \cos^2 \theta \right], \\ \tilde{\mathcal{N}}_{++;+0}^{Y_2} &= -\tilde{\mathcal{N}}_{--;0-}^{Y_2} = \tilde{\mathcal{N}}_{++;0+}^{Y_2} = -\tilde{\mathcal{N}}_{--;-0}^{Y_2} = -24\sqrt{\hat{r}}(\hat{\beta} + 1)(\hat{\beta} - 2) \cos \theta, \\ \tilde{\mathcal{N}}_{++;+-}^{Y_2} &= -\tilde{\mathcal{N}}_{--;+-}^{Y_2} = \tilde{\mathcal{N}}_{++;-+}^{Y_2} = -\tilde{\mathcal{N}}_{--;-+}^{Y_2} = -\frac{48}{\sqrt{6}}\hat{r}(1 + \hat{\beta}^2), \\ \tilde{\mathcal{N}}_{++;00}^{Y_2} &= -\tilde{\mathcal{N}}_{--;00}^{Y_2} = 96 \sin^2 \theta, \\ \tilde{\mathcal{N}}_{++;0-}^{Y_2} &= -\tilde{\mathcal{N}}_{--;+0}^{Y_2} = \tilde{\mathcal{N}}_{++;-0}^{Y_2} = -\tilde{\mathcal{N}}_{--;0+}^{Y_2} = 24\sqrt{\hat{r}}(\hat{\beta} - 1)(\hat{\beta} + 2) \cos \theta, \\ \tilde{\mathcal{N}}_{++;+-}^{Y_2} &= -\tilde{\mathcal{N}}_{--;+-}^{Y_2} = -12\hat{r} \left[ 1 + 3\hat{\beta} + \hat{\beta}^2 - \hat{\beta}^3 + (1 - \hat{\beta} - 3\hat{\beta}^2 - \hat{\beta}^3) \cos^2 \theta \right], \\ \tilde{\mathcal{N}}_{+-;++}^{Y_2} &= -\tilde{\mathcal{N}}_{+-;--}^{Y_2} = \tilde{\mathcal{N}}_{-+;++}^{Y_2} = -\tilde{\mathcal{N}}_{-+;--}^{Y_2} = \frac{48}{\sqrt{6}}\hat{r}(1 + \hat{\beta}^2), \\ \tilde{\mathcal{N}}_{+-;+0}^{Y_2} &= -\tilde{\mathcal{N}}_{+-;0-}^{Y_2} = \tilde{\mathcal{N}}_{-+;0+}^{Y_2} = -\tilde{\mathcal{N}}_{-+;-0}^{Y_2} = \tilde{\mathcal{N}}_{-+;+0}^{Y_2} \\ &= -\tilde{\mathcal{N}}_{-+;0-}^{Y_2} = \tilde{\mathcal{N}}_{-+;0+}^{Y_2} = -\tilde{\mathcal{N}}_{-+;-0}^{Y_2} = 24\sqrt{2\hat{r}}\hat{\beta}. \end{aligned} \quad (5.16)$$

The two contributions behave differently at high energies. The  $Y_1$  contributions are

dominant in the amplitudes for producing two longitudinal  $W$ 's from the  $J_Z = 0$  initial photon state

$$\tilde{\mathcal{N}}_{\pm\pm;00}^{Y_1} \rightarrow \mp 4\hat{r} \sin^2 \theta, \quad (5.17)$$

while the  $Y_2$  contributions are dominant in the amplitudes for producing two transverse  $W$ 's except for the  $(\pm\pm; \pm\pm)$  modes

$$\begin{aligned} \tilde{\mathcal{N}}_{\pm\pm;\mp\mp}^{Y_2} &\rightarrow \mp 48\hat{r} \sin^2 \theta, \\ \tilde{\mathcal{N}}_{\pm\pm;+-}^{Y_2} = \tilde{\mathcal{N}}_{\pm\pm;-+}^{Y_2} &\rightarrow \mp 16\sqrt{6}\hat{r}, \\ \tilde{\mathcal{N}}_{+-;\pm\pm}^{Y_2} = \tilde{\mathcal{N}}_{-+;\pm\pm}^{Y_2} &\rightarrow \pm 16\sqrt{6}\hat{r}. \end{aligned} \quad (5.18)$$

The high-energy behavior of two sets of amplitudes (5.15) and (5.16) are in sharp contrast to that of the SM amplitudes whose dominant contributions are in the  $(\pm\pm; \pm\pm)$ ,  $(\pm\mp; \pm\mp)$ , and  $(\pm\mp; 00)$  modes. Because of this, interference between different helicity amplitudes are essential to observe significant CP violation effects. Use of the linearly polarized photon beams allow us to study interference between the leading CP-even (SM) amplitudes and the leading CP-odd amplitudes. In our approximation of neglecting the one-loop  $\gamma\gamma H$  vertex of the SM, there is no contribution from the  $Y_3$  term;

$$\tilde{\mathcal{M}}^{Y_3} = 0. \quad (5.19)$$

On the other hand  $Y_4$  contributes to the  $s$ -channel scalar exchange diagram in the helicity amplitudes with  $\Delta\lambda_{12} = \Delta\lambda_{34} = 0$ . An explicit calculation shows that the non-vanishing amplitudes,  $\tilde{\mathcal{M}}_{Y_4}$ , are as follows;

$$\begin{aligned} \tilde{\mathcal{M}}_{++;++}^{Y_4} &= -\tilde{\mathcal{M}}_{--;--}^{Y_4} = 4\chi_H(\hat{s}), \\ \tilde{\mathcal{M}}_{++;00}^{Y_4} &= -\tilde{\mathcal{M}}_{--;00}^{Y_4} = -\hat{r}(1 + \hat{\beta}^2)\chi_H(\hat{s}), \\ \tilde{\mathcal{M}}_{++;--}^{Y_4} &= -\tilde{\mathcal{M}}_{--;++}^{Y_4} = 4\chi_H(\hat{s}), \end{aligned} \quad (5.20)$$

where  $\chi_H$  is the Higgs propagator factor

$$\chi_H(\hat{s}) = \frac{\hat{s}}{\hat{s} - m_H^2 + im_H \Gamma_H}. \quad (5.21)$$

In the subsequent numerical studies, we examine the case with  $m_H = 100$  GeV where the width  $\Gamma_H$  is safely neglected. We will study the  $m_H \geq 2m_W$  case elsewhere, since there both the tree- and one-loop SM amplitudes are relevant.

## VI. DIFFERENTIAL CROSS SECTION

In counting experiments where the final  $W$  polarizations are not analyzed, we measure only the following combinations:

$$\sum_X M_{\lambda_1 \lambda_2} M_{\lambda'_1 \lambda'_2}^* = e^4 \sum_{\lambda_3} \sum_{\lambda_4} \tilde{\mathcal{M}}_{\lambda_1 \lambda_2; \lambda_3 \lambda_4} \tilde{\mathcal{M}}_{\lambda'_1 \lambda'_2; \lambda_3 \lambda_4}^*. \quad (6.1)$$

We then find  $\Sigma_{\text{unpol}}$ ,  $\Sigma_{02}$ ,  $\Delta_{02}$ ,  $\Sigma_{22}$ , and  $\Sigma_{00}$  from Eq. (13). The differential cross section for a fixed angle  $\chi$  is

$$\begin{aligned} \frac{d^2\sigma}{d\cos\theta d\phi}(\chi) = & \frac{\alpha^2}{8\hat{s}(1 - \hat{\beta}^2 \cos^2 \theta)^2} \left\{ \hat{\Sigma}_{\text{unpol}} - \frac{1}{2} \text{Re} \left[ \left( \eta e^{-i(\chi+\phi)} + \bar{\eta} e^{-i(\chi-\phi)} \right) \hat{\Sigma}_{02} \right] \right. \\ & \left. + \frac{1}{2} \text{Re} \left[ \left( \eta e^{-i(\chi+\phi)} - \bar{\eta} e^{-i(\chi-\phi)} \right) \hat{\Delta}_{02} \right] + \eta \bar{\eta} \text{Re} \left[ e^{-2i\phi} \hat{\Sigma}_{22} + e^{-2i\chi} \hat{\Sigma}_{00} \right] \right\}, \end{aligned} \quad (6.2)$$

$$\Sigma_i = \frac{e^2 \hat{\Sigma}_i}{(1 - \hat{\beta}^2 \cos^2 \theta)^2}, \quad \Delta_{02} = \frac{e^2 \hat{\Delta}_{02}}{(1 - \hat{\beta}^2 \cos^2 \theta)^2}, \quad (6.3)$$

for  $i = \text{unpol}, 02, 22$ , and  $00$ .

We first note that all the real parts of the distributions (6.1) are independent of the anomalous CP-odd form factors  $Y_i$  up to linear order

$$\begin{aligned} \hat{\Sigma}_{\text{unpol}} &= 38 - 4\hat{\beta}^2(3 - 8\cos^2 \theta) + 6\hat{\beta}^4(1 + \sin^4 \theta), \\ \mathcal{R}(\hat{\Sigma}_{02}) &= \frac{96}{\hat{r}} \hat{\beta}^2 \sin^2 \theta, \quad \mathcal{R}(\hat{\Delta}_{00}) = 0, \\ \mathcal{R}(\hat{\Sigma}_{22}) &= 6\hat{\beta}^4 \sin^4 \theta, \quad \mathcal{R}(\hat{\Sigma}_{00}) = \frac{96}{\hat{r}^2}. \end{aligned} \quad (6.4)$$

On the other hand, two CP-odd distributions,  $\mathcal{I}(\hat{\Sigma}_{02})$  and  $\mathcal{I}(\hat{\Sigma}_{00})$ , have contributions from the  $Y_1$ ,  $Y_2$ , and  $Y_4$  terms



$$\mathcal{I}(\hat{\Sigma}_{02}) = -4\hat{r}\hat{\beta}^2 \left[ 4(1 - \hat{\beta}^2 \cos^2 \theta)R(Y_1) + 48(3 + \hat{\beta}^2 \cos^2 \theta)R(Y_2) \right. \\ \left. + (5 - 3\hat{\beta}^2)(1 - \hat{\beta}^2 \cos^2 \theta)R(Y_4\chi_H) \right] \sin^2 \theta, \quad (6.5)$$

$$\mathcal{I}(\hat{\Sigma}_{00}) = 24 \left[ 4R(Y_1) - 4\hat{r}(1 + 3\hat{\beta}^2)R(Y_2) + (1 + \hat{\beta}^2)R(Y_4\chi_H) \right] (1 - \hat{\beta}^2 \cos^2 \theta). \quad (6.6)$$

A few comments on the CP-odd distributions are in order.

- $\mathcal{I}(\hat{\Sigma}_{02})$  has  $\hat{\beta}^2$  as an overall factor such that the contribution vanishes at the threshold, whereas  $\mathcal{I}(\hat{\Sigma}_{00})$  does not.
- Both CP-odd distributions have the angular terms ( $\sin^2 \theta$  and  $1 - \hat{\beta}^2 \cos^2 \theta$ ) which become largest at the scattering angle  $\theta = \pi/2$ , where the SM contributions are generally small. We, therefore, expect large CP-odd asymmetries at  $\theta \approx \pi/2$ .
- Each term in  $\mathcal{I}(\Sigma_{02})$  has a different angular dependence which allows us to disentangle them. On the other hand, we note that all the terms in  $\mathcal{I}(\Sigma_{00})$  mode all the contributions have the same angular dependence. The only way to distinguish them is to study its energy dependence. We show that this can be efficiently done by adjusting the laser beam frequency in the Compton backscattering mode.
- At high energies ( $\hat{r} \gg 1$ ),  $R(Y_1)$  and  $R(Y_3)$  are measured from  $\mathcal{I}(\Sigma_{02})$ , whereas  $R(Y_2)$  affects both  $\mathcal{I}(\Sigma_{00})$  and  $\mathcal{I}(\Sigma_{02})$ .

## VII. OBSERVABLE CONSEQUENCES OF CP-ODD COUPLINGS

Let us estimate the various experimental branching fractions of  $W$  decays. Consider the decay of each  $W$  into a fermion-antifermion pair (quark-antiquark  $q_1\bar{q}_2$  or charged lepton-neutrino  $l\nu_l$ ) at tree level. The branching ratio for  $W^- \rightarrow l\bar{\nu}_l$  ( $l = e, \mu$ , or  $\tau$ ) is about 10% each [24]. We thus expect the following final state combinations:

$$\begin{aligned}
(q\bar{q})(q\bar{q}) &\Rightarrow 4\text{jets} && 49\%, \\
(q\bar{q})(l\nu) &\Rightarrow \text{dijet} + l^\pm + \cancel{p} && 42\%, \\
(l\bar{\nu})(\bar{l}\nu) &\Rightarrow l^+l^- + \cancel{p} && 9\%,
\end{aligned} \tag{7.1}$$

where  $\cancel{p}$  stands for the momentum of the escaping neutrino(s). The dijet+ $l^\pm$  mode is most amenable for  $W$ -spin analysis. In our analysis, no spin analysis for the decaying  $W$ 's is required. In case of  $\mathcal{I}(\Sigma_{00})$ , not even the scattering plane needs to be identified. Even if one excludes the  $\tau^+\tau^- + \cancel{p}$  modes of 1%, the remaining 99% of the events can be used to measure  $\mathcal{I}(\Sigma_{00})$ . On the other hand, the scattering plane should be identified to measure  $\mathcal{I}(\Sigma_{02})$ . It is worth noting that the charge of the decaying  $W$  is not needed to extract  $\mathcal{I}(\Sigma_{02})$ . Therefore all the modes except for the  $l^+l^- + \cancel{p}$  modes (9%) can be used for  $\mathcal{I}(\Sigma_{02})$ .

The  $\gamma\gamma \rightarrow W^+W^-$  reaction has a much larger cross section than heavy fermion-pair production such as  $\gamma\gamma \rightarrow t\bar{t}$  and, furthermore, the total cross section approaches a constant value at high c.m. energies. At  $\sqrt{\hat{s}} = 500$  GeV the total cross section is about 80 pb, while the  $t\bar{t}$  cross section is about 1 pb. So there exist no severe background problems. In the following analysis we simply assume that all the  $W$  pair events can be used. It would be rather straightforward to include the effects from any experimental cuts and efficiencies in addition to the branching factors discussed above.

We present our numerical analysis at the following set of collider parameters:

$$\sqrt{s} = 0.5 \text{ and } 1.0 \text{ TeV}, \quad \kappa^2 \cdot L_{ee} = 20 \text{ fb}^{-1}. \tag{7.2}$$

The dimensionless parameter  $x$ , which is dependent on the laser frequency  $\omega_0$ , is treated as an adjustable parameter. We note that  $\kappa = 1$  is the maximally allowed value for the  $e\text{-}\gamma$  conversion coefficient  $\kappa$  and it may be as small as  $\kappa = 0.1$  if the collider is optimized for the  $e^+e^-$  model [14]. All one should note is that the significance of the signal scales as  $(\epsilon \cdot \kappa^2 \cdot L_{ee})$ , where  $\epsilon$  denotes the overall detection efficiency that is different for  $A_{00}$  and  $A_{02}$ .

### A. Statistical significance of possible signals

The two CP-odd integrated asymmetries,  $A_{00}$  and  $A_{02}$ , depend linearly on the form factors,  $R(Y_1)$ ,  $R(Y_2)$ , and  $R(Y_4)$  in the approximation that only the terms linear in the form factors are retained. We present the sensitivities to each form factor, assuming that the other form factors are zero. The analyses are catalogued into two parts: the  $\gamma(\gamma)WW$  part and the  $\gamma\gamma H$  part.

Folding the photon luminosity spectrum and integrating the distributions over the polar angle  $\theta$ , we obtain the  $x$ -dependence of available event rates:

$$\begin{pmatrix} N_{\text{unpol}} \\ N_{02} \\ N_{00} \end{pmatrix} = \kappa^2 L_{ee} \frac{\pi \alpha^2}{2s} \int_{\tau_{\min}}^{\tau_{\max}} \frac{d\tau}{\tau} \int_{-1}^1 d\cos\theta \frac{\hat{\beta} \langle \phi_0 \phi_0 \rangle_{\tau}}{(1 - \hat{\beta}^2 \cos^2 \theta)^2} \begin{pmatrix} \hat{\Sigma}_{\text{unpol}} \\ \mathcal{A}_{\eta} \mathcal{I}(\hat{\Sigma}_{02}) \\ \mathcal{A}_{\eta\eta} \mathcal{I}(\hat{\Sigma}_{00}) \end{pmatrix}, \quad (7.3)$$

where  $\tau_{\max} = (x/(1+x))^2$  and  $\tau_{\min} = 4m_W^2/s$ . One measure of the significance of a CP-odd asymmetry is the standard deviation  $\mathcal{N}_{SD}^a$  by which the asymmetry exceeds the expected statistical fluctuation of the background distribution; for  $a = 02$  and  $00$

$$\mathcal{N}_{SD}^a = \frac{|A_a|}{\sqrt{2/\epsilon N_{\text{unpol}}}}. \quad (7.4)$$

Here  $\epsilon$  is for the sum of  $W$  branching fractions available, which is taken to be

$$\epsilon = \begin{cases} 100\% & \text{for } N_{00}, \\ 91\% & \text{for } N_{02}. \end{cases} \quad (7.5)$$

Separating the asymmetry  $A_a$  into four independent parts as

$$A_a = R(Y_1)A_a^{Y_1} + R(Y_2)A_a^{Y_2} + R(Y_4)A_a^{Y_4}, \quad (7.6)$$

and considering each form factor separately, we obtain the  $1\text{-}\sigma$  allowed upper bounds of the form factors ( $i = 1, 2, 4$ )

$$\text{Max}(|R(Y_i)|_a) = \frac{\sqrt{2}}{|A_a^{Y_i}| \sqrt{\epsilon N_{\text{unpol}}}}, \quad (7.7)$$

if no asymmetry is found. The  $N_{SD}\text{-}\sigma$  upper bound is determined simply by multiplying  $\text{Max}(|R(Y_i)|_a)$  and  $\text{Max}(|I(Y_4)|_a)$  by  $N_{SD}$ .

### B. The $\gamma WW$ and $\gamma\gamma WW$ vertices: $Y_1$ and $Y_2$

The parity-violating form factors  $Y_1$  and  $Y_2$  respect charge conjugation invariance and they are related to the  $W$  electric dipole moment(EDM)  $d_W$  and the  $W$  magnetic quadrupole moment(MQD)  $\tilde{Q}_W$  of  $W^+$  by

$$d_W = \frac{2e}{m_W} (Y_1 + 6Y_2), \quad \tilde{Q}_W = -\frac{4e}{m_W^2} (Y_1 - 6Y_2). \quad (7.8)$$

There are strong indirect phenomenological constraints on the above couplings arising from the EDM of the electron and neutron [23]. However, we should note that there is a possibility of cancellation among different contributions which renders these indirect constraints ineffective. Direct studies of  $W$ -pair production at high energies are quite complementary to the precision experiments at low energies. Although the interplay between high- and low-energy experimental constraints is important, the latter constraints can not replace the role of high-energy experiments.

Figs.4(a) and (b) show the  $x$  dependence of the sensitivities to  $R(Y_1)$ , which are obtained from  $A_{02}$  and  $A_{00}$ , respectively, for  $\sqrt{s} = 0.5$  TeV and  $\sqrt{s} = 1$  TeV. The  $x$  dependence of the sensitivities to  $R(Y_2)$  are shown in Figs. 5(a) and (b). In both figures, the solid lines are for  $\sqrt{s} = 0.5$  TeV and the long-dashed lines for  $\sqrt{s} = 1.0$  TeV. Let us make a few comments on the results shown in the two figures (Figs. 4 and 5) and Table 4.

- The sensitivities, especially from the asymmetry  $A_{00}$  mode, depend strongly on the value of  $x$ . For smaller  $x$  values are favored for  $A_{00}$ , while relatively large  $x$  values favored for  $A_{02}$ . This property can be clearly understood by noting that  $\hat{A}_{00}$  gets suppressed as the  $\gamma\gamma$  c.m. energy increases, while  $\hat{A}_{02}$  does not.
- The optimal sensitivities on  $R(Y_2)$  are very much improved as the  $e^+e^-$  c.m. energy increases from 0.5 TeV to 1 TeV while those of  $R(Y_1)$  are a little improved. The optimal  $x$  values are reduced as the c.m. energy increases.
- At the two  $\sqrt{s}$  values the asymmetries  $A_{00}^{Y_1}$  gives stronger sensitivities than  $A_{02}^{Y_1}$  to  $R(Y_1)$ , while the two symmetries  $A_{02}^{Y_2}$  and  $A_{00}^{Y_2}$  gives rather similar sensitivities to  $R(Y_2)$ .

These properties can be understood from the  $\hat{s}$  dependence of the corresponding CP-odd distributions (6.6).

TABLE IV. The best  $1\text{-}\sigma$  bounds of the CP-odd form factors,  $R(Y_1)$  and  $R(Y_2)$ , and their corresponding  $x$  values for  $\sqrt{s} = 0.5$  and 1 TeV.

	$A_{02}$		$A_{00}$	
$\sqrt{s}$ (TeV)	0.5	1.0	0.5	1.0
$x$	1.83	0.96	0.75	0.31
$\text{Max}( R(Y_1) )$	$1.1 \times 10^{-2}$	$5.0 \times 10^{-3}$	$3.2 \times 10^{-3}$	$2.2 \times 10^{-3}$
$x$	2.09	1.23	1.11	0.59
$\text{Max}( R(Y_2) )$	$2.4 \times 10^{-4}$	$9.0 \times 10^{-5}$	$2.6 \times 10^{-4}$	$1.1 \times 10^{-4}$

The above results underlie the importance of having adjustable laser frequencies, which allows us to select the regime where each contribution becomes dominant. We find that the two-photon mode allows us to reach the limit that  $R(Y_1)$  is of the order of  $10^{-3}$  and  $R(Y_2)$  is of the order of  $10^{-4}$  or less.

### C. The $\gamma\gamma H$ vertex: $Y_4$

The  $\gamma\gamma H$  vertex  $Y_4$  can be studied in the process  $\gamma\gamma \rightarrow H$  [4], where the interference between the 1-loop SM amplitudes and the new CP-odd amplitudes lead to observable CP-odd asymmetries. In this paper, we study the sensitivity of the process  $\gamma\gamma \rightarrow W^+W^-$  to the CP-odd  $\gamma\gamma H$  coupling  $Y_4$  where  $m_H$  is below the  $W$ -pair threshold. For an actual numerical analysis we set  $m_H = 100$  GeV and assume that its width is negligible. Our results are insensitive to  $m_H$  as long as  $m_H < 2m_W$ .

TABLE V. The  $1\text{-}\sigma$  sensitivities to the CP-odd form factor,  $R(Y_4)$ , and their corresponding  $x$  values for  $\sqrt{s} = 0.5$  and 1 TeV. Here,  $m_H = 100$  GeV.

	$A_{02}$		$A_{00}$	
$\sqrt{s}$ (TeV)	0.5	1.0	0.5	1.0
$x$	1.43	0.69	0.76	0.31
$\text{Max}( R(Y_4) )$	$1.1 \times 10^{-2}$	$6.4 \times 10^{-3}$	$7.5 \times 10^{-3}$	$5.0 \times 10^{-3}$

The best sensitivities to  $R(Y_4)$  from the asymmetries  $A_{02}$  and  $A_{00}$  and their corresponding  $x$  values for  $\sqrt{s} = 0.5$  and 1.0 TeV are listed in Table 5. Two asymmetries give the approximately same sensitivities at the same  $x$  value. The doubling of the  $e^+e^-$  c.m. energy improves the sensitivity so much and renders the optimal  $x$  values smaller than those at  $\sqrt{s} = 0.5$  TeV. Fig. 6 show the very strong  $x$  dependence of the  $R(Y_4)$  1- $\sigma$  sensitivities. Quantitatively we find that the constraints on  $R(Y_4)$  are of the order of  $10^{-3}$  for  $m_H = 100$  GeV at  $\sqrt{s} = 0.5$  and 1.0 TeV.

#### D. Model expectations

In order to assess the usefulness of the two-photon mode with polarized photons it is useful to estimate the expected size of the CP-odd form factors in a few specific models with reasonable physics assumptions. Several works [22] have estimated the size of the  $W$  EDM in various models beyond the SM. They have shown that the  $W$  EDM can be of the order  $10^{-20}$  (ecm) in the multi-Higgs-doublet model and the supersymmetric SM, corresponding to  $Y_1$  and  $Y_2$  of the order of  $10^{-4}$ . It is predicted of about  $10^{-22}$  and less than  $10^{-38}$  (ecm) in the left-right model and the SM, respectively,

In more general, if these vertices appear in the one-loop level [26] the coefficients  $f_i$  may contain a factor of  $1/16\pi^2$ . By setting all  $f_i$ 's to be  $1/16\pi^2$  and setting  $\Lambda = v = 246$  GeV, we find

$$|Y_1| \sim |Y_3| \sim |Y_4| \sim 10^{-3}, \quad |Y_2| \sim 10^{-4}. \quad (7.9)$$

The above order of magnitude estimates (7.9) of the form factors are consistent with the values expected in some specific models.

It is worth remarking that the two-photon experiments may allow us to probe the CP-odd effects of the expected size (7.9). The two-photon collider with polarized photons and adjustable laser frequency can play a crucial role in probing CP violation in the bosonic sector.

### **E. Comparison of the $\gamma\gamma$ mode and the $e^+e^-$ mode**

The initial  $e^+e^-$  state of the  $e^+e^- \rightarrow W^+W^-$  process is (almost) CP-even due to the very small electron mass. It is then clear that the initial electron beam polarizations are not so useful to construct large CP-odd asymmetries. CP-violating  $W$  interactions can be probed only via spin/angular correlations of the decaying  $W$ 's. For  $L_{ee} = 20 \text{ fb}^{-1}$  and  $\kappa = 1$ , we compare the constraints from the two-photon mode with those from the  $e^+e^-$  mode by studying the  $W^\pm$  decay correlations at  $\sqrt{s} = 0.5 \text{ TeV}$ .

The process  $e^+e^- \rightarrow W^+W^-$  [11,13] has been investigated in detail. For the present comparison let us refer to the work by Kalyniak, *et.al* [13], where they have assumed  $L_{ee} = 50 \text{ fb}^{-1}$  and a perfect detector. Readjusting the  $e^+e^-$  integrated luminosity to  $20 \text{ fb}^{-1}$ , we can summarize their findings; the total cross section with the pure leptonic decay modes of the  $W$ 's gives the constraint  $|R(Y_1)| \leq 5 \times 10^{-2}$ . below the expected level of statistical precision of approximately The two-photon mode is much more promising than the  $e^+e^-$  mode in probing CP violation in the  $W$  pair production, if  $\kappa \sim 1$   $e\gamma$  conversion rate is technically achieved.

## **VIII. SUMMARY AND CONCLUSIONS**

In this paper we have made a systematic study of observable asymmetries related with two polarized-photon collisions via the Compton backscattered laser beam at future linear colliders, which could serve as tests of possible CP-violating effects. We have described in a general framework how photon polarization is employed to study CP invariance in the initial

two-photon state. We have considered the most general dimension-six CP-odd operators in the scalar and vector boson sector, preserving all the SM gauge symmetries in the linear realization of the electroweak symmetry breaking.

Limiting ourselves to purely linearly-polarized photon beams, we have constructed two CP-odd asymmetries in the process  $\gamma\gamma \rightarrow W^+W^-$ . The CP-odd asymmetries can be extracted by simply adjusting the angle between the polarization vectors of two laser beams. We have found that the sensitivities of the CP-odd asymmetries to the CP-odd form factors depend strongly on the  $e^+e^-$  c.m. energy and the laser beam frequency.

In Tables 4 and 5 the maximal sensitivities of the CP-odd form factors and the corresponding  $x$  values have been shown for  $\sqrt{s} = 0.5$  and 1 TeV with  $\kappa^2 \cdot L_{ee} = 20 \text{ fb}^{-1}$ . The sensitivities are high enough to probe CP-odd new interactions beyond the limits from some specific models with reasonable physics assumptions.

We have found that, for  $\kappa \sim 1$ , a counting experiment in the two-photon mode with adjustable laser frequency can give much stronger constraints on the  $W$  EDM and magnetic quadratic moment (MQD) than the  $e^+e^-$  mode can do through the  $W^\pm$  decay correlations in  $e^+e^-$  collisions using a perfect detector.

To conclude, (linearly) polarized photons by backscattered laser beams of adjustable frequencies at a TeV scale  $e^+e^-$  linear  $e^+e^-$  collider provide us with a very efficient mechanism to probe CP violation in two-photon collisions.

## ACKNOWLEDGEMENTS

The authors would like to thank F. Boudjema, F. Cuypers, I.F. Ginzburg, H.S. Song, R. Szalapski, T. Takahashi, C.P. Yuan, and P.M. Zerwas for useful suggestions and helpful comments. The work of SYC is supported in part by the Japan Society for the Promotion of Science (No. P-94024) and that of KH by the Grant-in-Aid for Scientific Research from the Japanese Ministry of Education, Science and Culture (No. 05228104). The work of MSB is supported by Center for Theoretical Physics, Seoul National University.



## REFERENCES

- [1] M. Kobayashi and T. Maskawa, Prog. Theor. Phys. **49**, 379 (1973).
- [2] Proceedings of the 1st International Workshop on “Physics and Experiments with Linear  $e^+e^-$  Colliders” (Saariselka, Finland, September 1991), eds. R. Orava, P. Eerola, and M. Nordberg (World Scientific, Singapore, 1992); Proceedings of the 2nd International Workshop on “Physics and Experiments with Linear  $e^+e^-$  Colliders” (Waikoloa, Hawaii, April 1993), eds. F.A. Harris, S.L. Olsen, S. Pakvasa, and X. Tata (World Scientific, Singapore, 1993).
- [3] S.Y. Choi and F. Schrempp, Phys. Lett. B272, 149 (1991); E. Yehudai, Phys. Rev. D **44**, 3434 (1991); Ph. D Thesis, SLAC-PUB-383; F. Boudjema and G. Bélanger, Phys. Lett. B288, 288 (1992); Proceedings of the Workshop on Gamma-Gamma Colliders (LBL, Berkely, 1994), eds. S. Chattopadhyay and A.M. Sessler, Nucl. Instr. and Meth. A 355 (1995); M. Baillargeon, G. Bélanger, and F. Boudjema, in the Proceedings of Two-Photon Physics from DAΦNE to LEP200 and Beyond, (Paris, 1994).
- [4] J.F. Gunion and H.E. Haber, Phys. Rev. D **48**, 5109 (1993); P.M. Zerwas, in the Proceedings of the VIII Int. Workshop on Photon-Photon Collisions, Shresh (Jerusalem Hills) 1988; S.J. Brodsky, in the Proceedings of the Workshop on “Physics and Experiments with Linear  $e^+e^-$  Colliders” (Waikoloa, Hawaii, April 1993), eds. F.A. Harris, S.L. Olsen, S. Pakvasa, and X. Tata (World Scientific, Singapore, 1993); J.F. Gunion, *ibid.*; D.L. Borden, D.A. Bauer, and D.O. Caldwell, SLAC-PUB-5715; Phys. Rev. D **48**, 4018 (1993).
- [5] B. Graadkowski and J.F. Gunion, Phys. Lett. B291, 361 (1992); M. Krämer, J. Kühn, M.L. Stong, and P.M. Zerwas, Z. Phys. C **64**, 21 (1994); J.F. Gunion and J.G. Kelly, UCD-94-21 and hep-ph-9404343.
- [6] W. Bernreuther and A. Brandenburg, Phys. Lett. B314, 104 (1993); W. Bernreuther,

- J.P. Ma, and B.H.J. McKellar, Phys. Rev. D **51**, 2475 (1995); H. Anlauf, W. Bernreuther, and A. Brandenburg, PITHA 95/11, hep-ph-9504424 and refereces therein.
- [7] J.P. Ma and B.H.J. McKellar, Phys. Lett. B319 (1993) 533.
- [8] G. Bélanger and G. Couture, Phys. Rev. D49 (1994) 5720.
- [9] S.Y. Choi and K. Hagiwara, Phys. Lett. B359 (1995) 369.
- [10] K. Hikasa, Phys. Lett. B143, 266 (1984); Phys. Rev. D **33**, 3203 (1986).
- [11] K. Hagiwara, R.D. Peccei, D. Zeppenfeld and K. Hikasa, Nucl. Phys. B282 (1987) 253.
- [12] G. Gounaris, D. Schildknecht, and F.M. Renard, Phys. Lett. B263, 291 (1991); M.B. Gavela, F. Iddir, A. Le Yaouanc, L. Oliver, O. Pène, and J.C. Raynal, Phys. Rev. D **39**, 1870 (1989); A. Bilal, E. Massó, and A. De Rújula, Nucl. Phys. **B355**, 549 (1991); G. Gounaris, J.L. Kneur, J. Layssac, G. Moultaka, F.M. Renard, and D. Schildknecht, in the Proceedings of  $e^+e^-$  Collisions at 500 GeV: The Physics Potential, Part C , ed. P.M. Zerwas, DESY 93-123 C, 735 (1993).
- [13] P. Kalyniak, P.Madsen, N. Sinha, and R. Sinha, Phys. Rev. D **52**, 3826 (1995).
- [14] I.F. Ginzburg, G.L. Kotkin, V.G. Serbo, S.L. Panfil and V.I. Telnov, Sov. ZhETF Pis'ma **34**, 514 (1981) [JETP Lett. **34**, 491 (1982)]; Nucl. Instr. and Meth. **205**, 47 (1983); I.F. Ginzburg, G.L. Kotkin, S.L. Panfil, V.G. Serbo, and V.I. Telnov, *ibid* **219**, 5 (1984); V.I. Telnov, *ibid* **A294**. 72 (1992); Proceedings of the 1st Workshop on “Physics and Experiments with Linear  $e^+e^-$  Colliders” (Saariselka, Filand, September 1991), eds. R. Orava, P. Eerola, and M. Nordberg (World Scientific, Singapore, 1992); D.L. Borden, Proceedings of the 2st Workshop on “Physics and Experiments with Linear  $e^+e^-$  Colliders” (Waikoloa, Hawaii, April 1993), eds. F.A. Harris, S.L. Olsen, S. Pakvasa, and X. Tata (World Scientific, Singapore, 1993).
- [15] V.B. Berestetskii, E.M Lifshitz, and L.P. Pitaevskii, *Relativistic Quantum Theory*,

- (Pergamon, Oxford, 1971), Part I, Chap. 1.
- [16] W. Buchmüller and D. Wyler, Nucl. Phys. B268, 621 (1986); C.J.C. Burgess and H.J. Schnitzer, *ibid* **B228**, 464 (1983); C.N. Leung, S.T. Love and S. Rao, Z. Phys. **C31**, 433 (1986).
  - [17] K. Hagiwara and M. Stong, Z. Phys. **C62** (1994) 99.
  - [18] The authors in Ref. [8] also has considered the distribution  $\mathcal{I}(\Sigma_{02})$ , but not the distribution  $\mathcal{I}(A_{00})$ .
  - [19] The function  $A_{\eta\eta}$  has been considered by M. Krämer, *et al.* in Ref. [5].
  - [20] J. Wudka, Nucl. Phys. Proc. Suppl. 37A (1994) 211.
  - [21] J.F. Gunion, H.E. Haber, G. Kane, and S. Dawson, *Higgs Hunter's Guide*, (Addison-Wesley, Redwood City, CA, 1990).
  - [22] D. Chang, W.Y. Keung and J. Liu, Nucl. Phys. B355 (1991) 295; R. López-Mobilia and T.H. West, Phys. Rev. D51 (1995) 6495.
  - [23] W. Marciano and A. Queijeiro, Phys. Rev. D **33**, 3449 (1986); F. Boudjema, K. Hagiwara, C. Hamzaoui, and K. Numata, *ibid* D **43**, 2223 (1991); A. De Rijula, M. Gavela, O. Pène, and F. Vegas, Nucl. Phys. **B357**, 311 (1991); see also S. Barr and W. Marciano, *CP Violation*, ed. C. Jarlskog (World Scientific, Singapore, 1989).
  - [24] Particle Data Group, L. Montanet *et al.*, Phys. Rev. D **50**, 1173 (1994).
  - [25] See, for example, Hagiwara, *et al.* in Ref. [11].
  - [26] C. Arzt, M.B. Einhorn and J. Wudka, Nucl. Phys. **B433**, 41 (1995) and references therein.

## FIGURES

FIG. 1. The coordinate system in the colliding  $\gamma\gamma$  c.m. frame. The scattering angle,  $\theta$ , and the azimuthal angles,  $\phi_1$  and  $\phi_2$ , for the linear polarization directions measured from the scattering plane are given.

FIG. 2. (a) the photon energy spectrum and (b) the degree of linear polarization of the Compton backscattered photon beam for  $x = 4E\omega_0/m_e^2 = 0.5, 1$  and  $4.83$ .

FIG. 3. (a) the  $\gamma\gamma$  luminosity spectrum and (b) the two linear polarization transfers,  $A_\eta$  (solid lines) and  $A_{\eta\eta}$  (dashed lines), for  $x = 4E\omega_0/m_e^2 = 0.5, 1$  and  $4.83$ .

FIG. 4. The  $x$  dependence of the  $R(Y_1)$  upper bound,  $\text{Max}(|R(Y_1)|)$ , at  $\sqrt{s} = 0.5$  and  $1.0$  TeV, from (a) the asymmetry  $A_{02}$  and (b) the asymmetry  $A_{00}$ , respectively. The solid lines are for  $\sqrt{s} = 0.5$  TeV and the long-dashed lines for  $\sqrt{s} = 1.0$  TeV.

FIG. 5. The  $x$  dependence of the  $R(Y_2)$  upper bound,  $\text{Max}(|R(Y_2)|)$  at  $\sqrt{s} = 0.5$  and  $1.0$  TeV, from (a) the asymmetry  $A_{02}$  and (b) the asymmetry  $A_{00}$ , respectively. The solid lines are for  $\sqrt{s} = 0.5$  TeV and the long-dashed lines for  $\sqrt{s} = 1.0$  TeV.

FIG. 6. The  $x$  dependence of the  $R(Y_4)$  upper bound,  $\text{Max}(|R(Y_4)|)$  at  $\sqrt{s} = 0.5$  and  $1.0$  TeV, from (a) the asymmetry  $A_{02}$  and (b) the asymmetry  $A_{00}$ , respectively. Here, the Higgs mass is  $m_H = 100$  GeV. The solid lines are for  $\sqrt{s} = 0.5$  TeV and the long-dashed lines for  $\sqrt{s} = 1.0$  TeV.

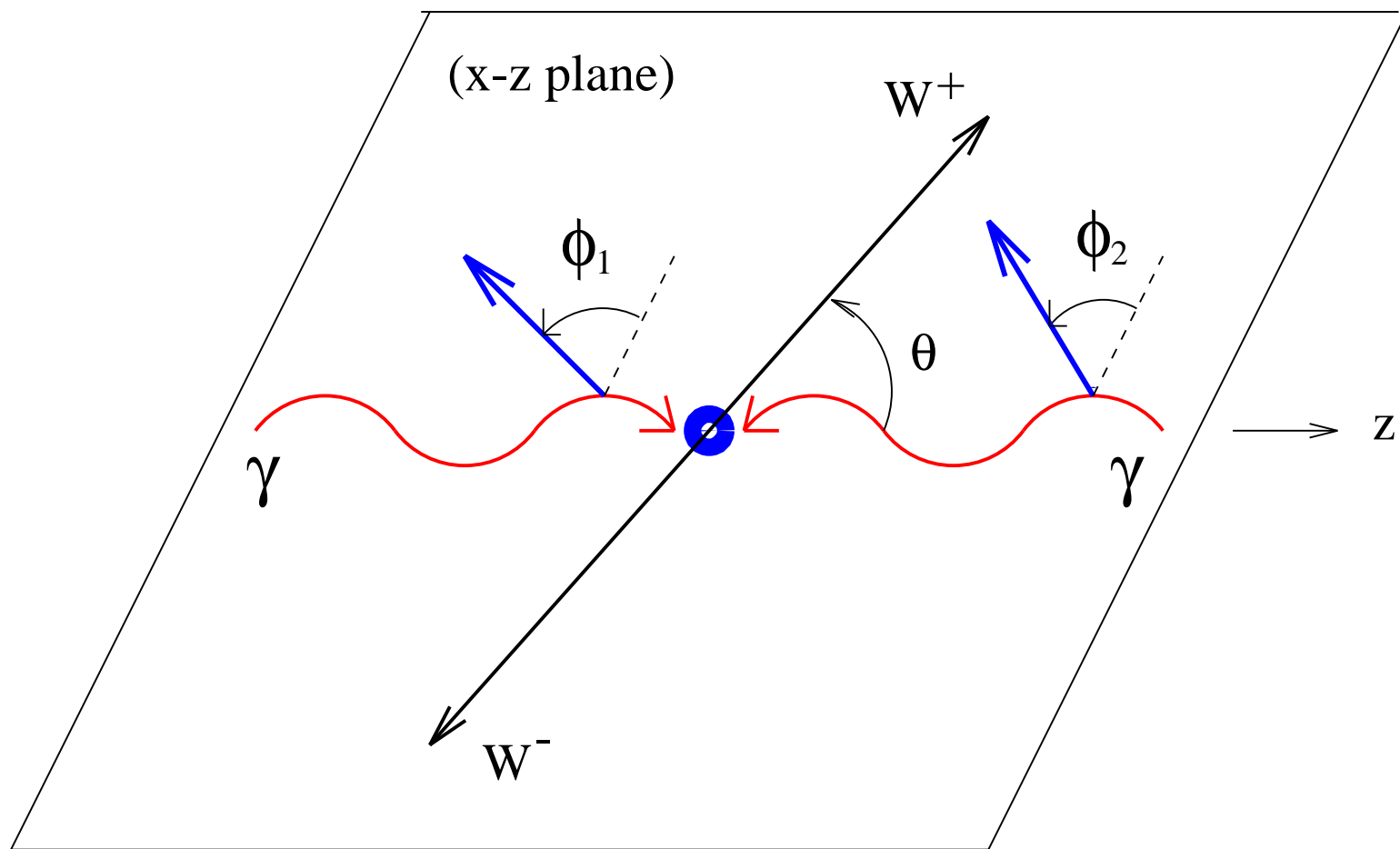
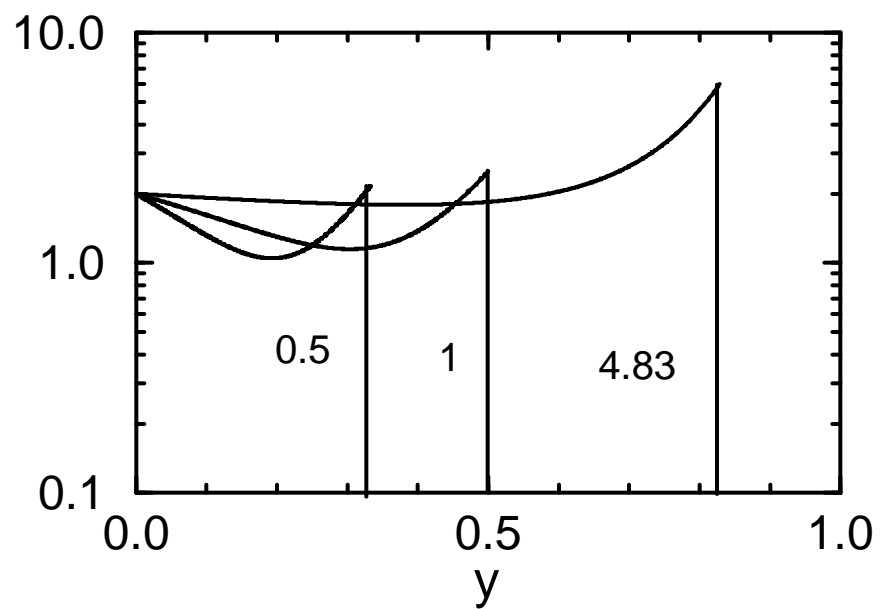


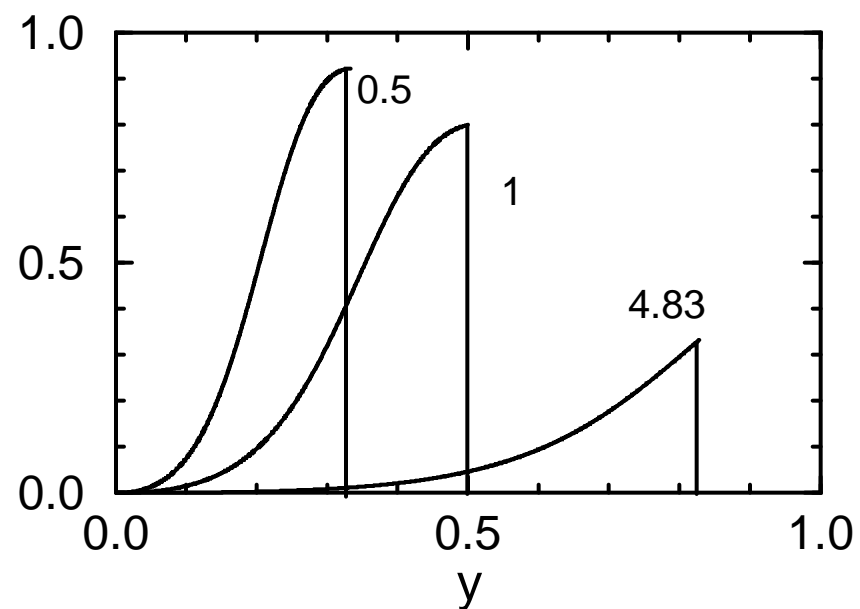
Fig. 1

Photon Spectrum



(a)

Linear Polarization



(b)

Fig. 2

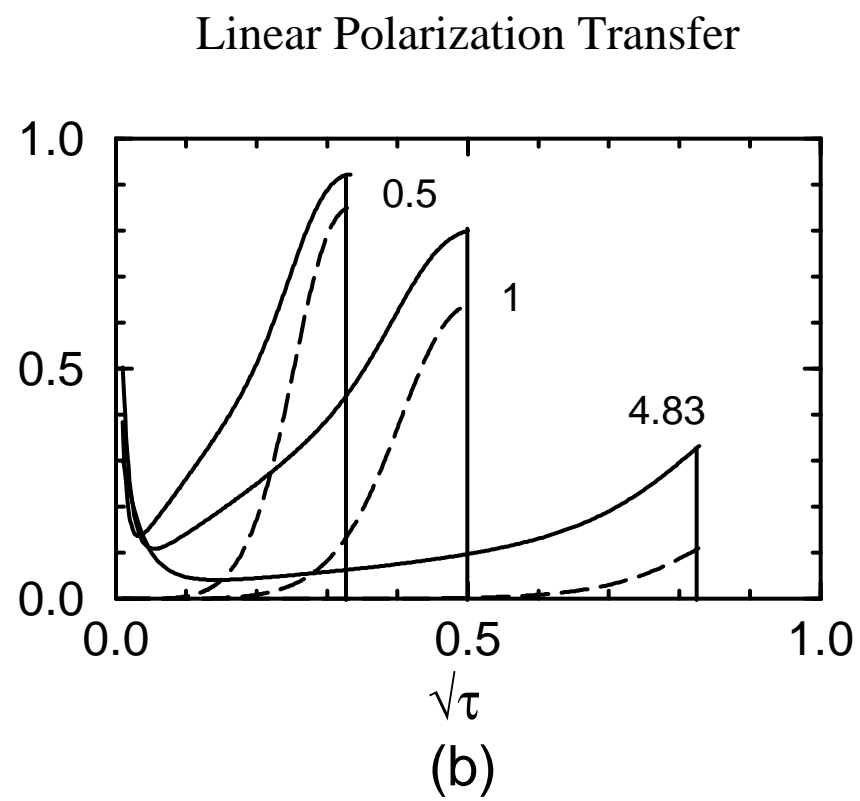
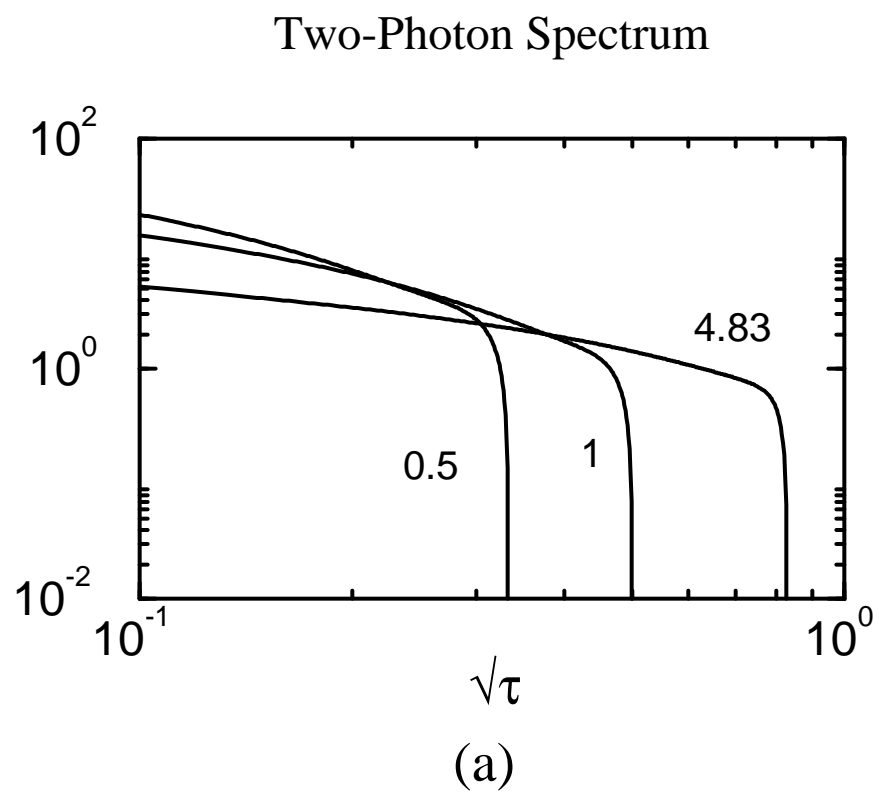


Fig. 3

$R(Y_1)$

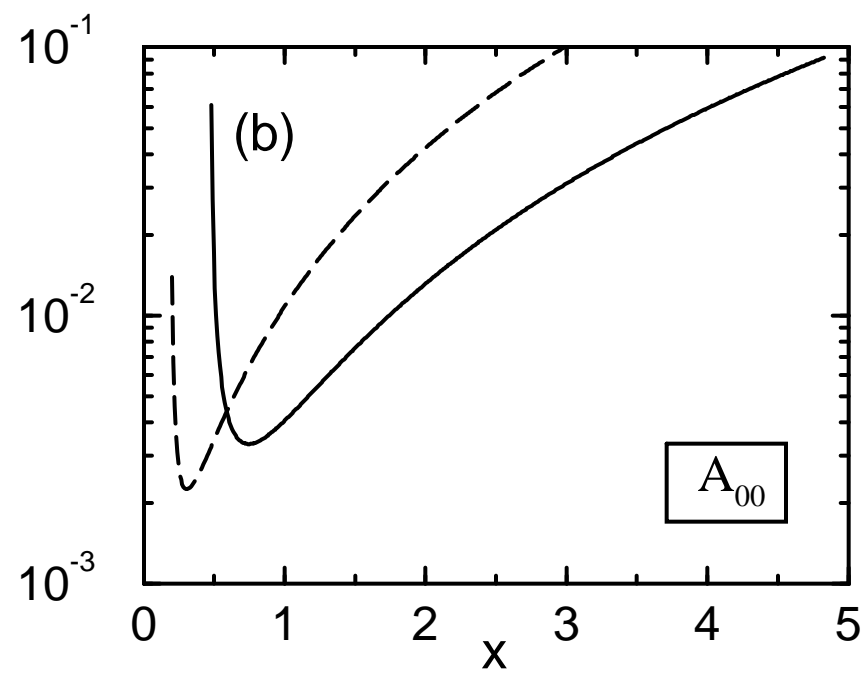
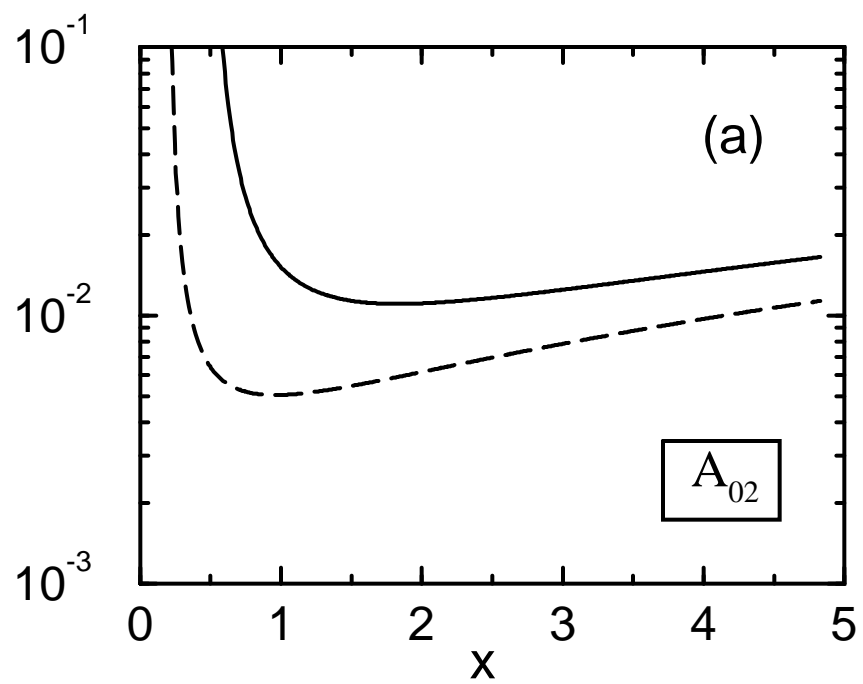


Fig. 4



$R(Y_2)$

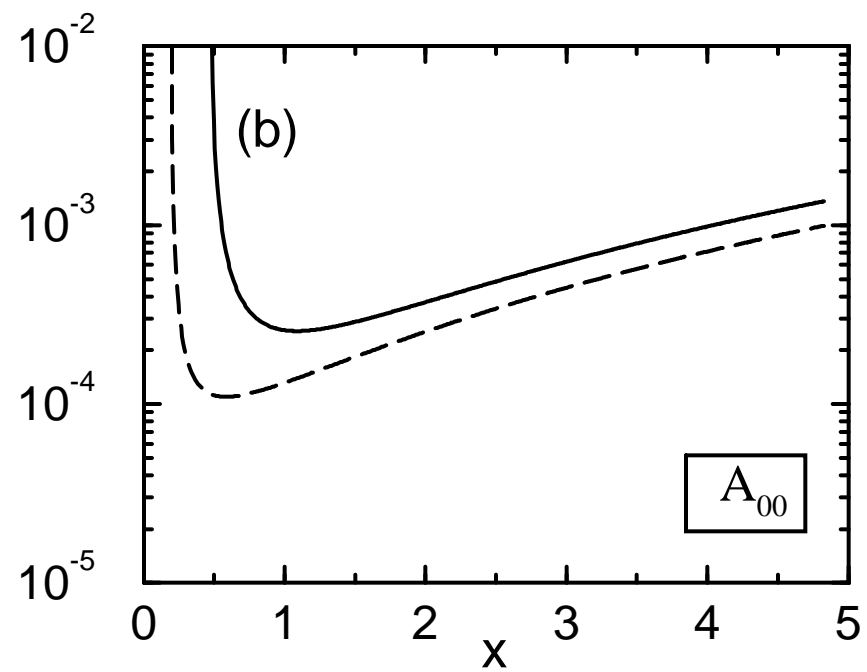
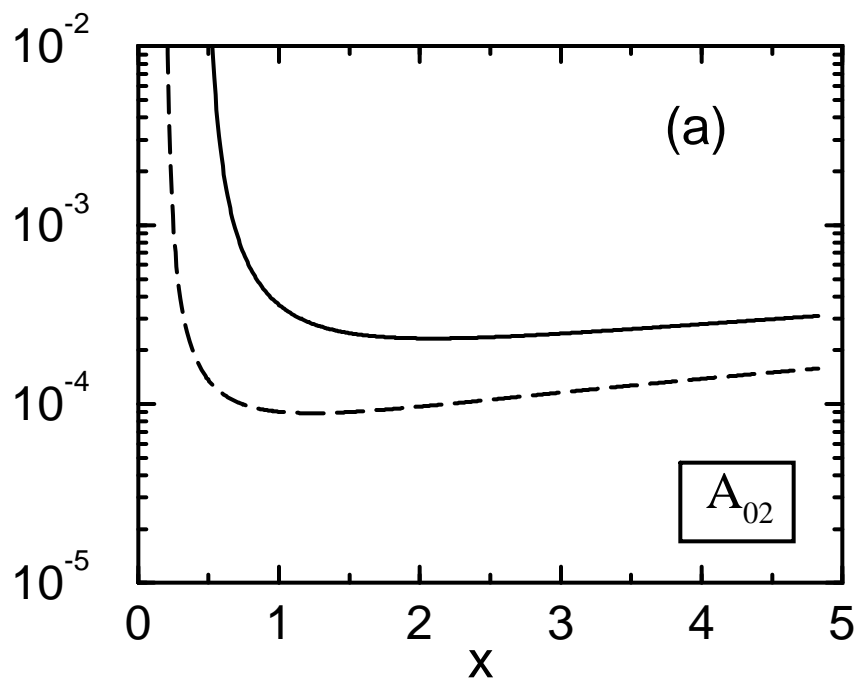


Fig. 5

$R(Y_4)$

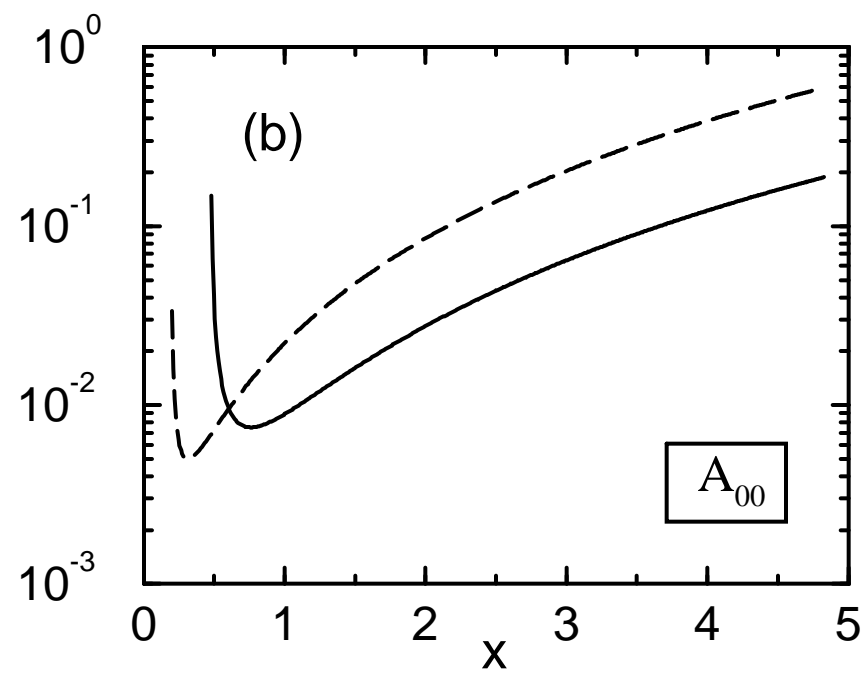
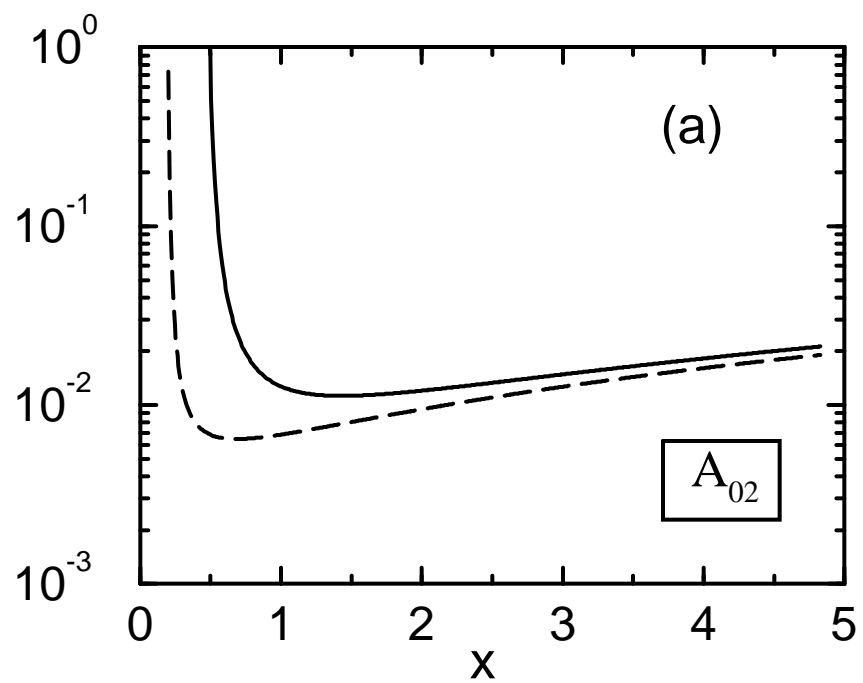


Fig. 6